Journal of Neurochemistry JNC

JOURNAL OF NEUROCHEMISTRY | 2009 | 110 | 496–508 doi: 10.1111/j.1471-4159.2009.06099.x

Tumor necrosis factor receptor-associated protein 1 regulates cell adhesion and synaptic morphology via modulation of N-cadherin expression

Kyoko Kubota,*,[1] Kiyoshi Inoue,*,†,[1] Ryota Hashimoto,‡,§,¶ Natsuko Kumamoto,* Asako Kosuga,** Masahiko Tatsumi,** Kunitoshi Kamijima,** Hiroshi Kunugi,¶ Nakao Iwata,†† Norio Ozaki,‡‡ Masatoshi Takeda§ and Masaya Tohyama*

*Department of Anatomy and Neuroscience, Osaka University Graduate School of Medicine, Suita, Osaka, Japan

†Center for Behavioral Neuroscience, Yerkes National Primate Research Center, Emory University, Atlanta, Georgia, USA

‡The Osaka-Hamamatsu Joint Research Center for Child Mental Development, Osaka University Graduate School of Medicine, Suita, Osaka, Japan

§Department of Psychiatry, Osaka University Graduate School of Medicine, Suita, Osaka, Japan

¶Department of Mental Disorder Research, National Institute of Neuroscience, National Center of Neurology and Psychiatry, Kodaira, Tokyo, Japan

**Department of Psychiatry, Showa University School of Medicine, Shinagawaku, Tokyo, Japan

††Department of Psychiatry, Fujita Health University School of Medicine, Toyoake, Aichi, Japan

‡‡Department of Psychiatry, Nagoya University Graduate School of Medicine, Nagoya, Aichi, Japan

Abstract

An increase in serum tumor necrosis factor-α (TNF-α) levels is closely related to the pathogenesis of major depression. However, the underlying molecular mechanism between this increase and impairment of brain function remains elusive. To better understand TNF-α/TNF receptor 1 signaling in the brain, we analyzed the brain distribution and function of tumor necrosis factor receptor-associated protein 1 (TRAP1). Here we show that TRAP1 is broadly expressed in neurons in the mouse brain, including regions that are implicated in the pathogenesis of major depression. We demonstrate that small interfering RNA-mediated knockdown of TRAP1 in a neuronal cell line decreases tyrosine phosphorylation of STAT3, followed by a reduction of the transcription factor E2F1, resulting in a down-regulation of N-cadherin, and affects the adhesive properties of the cells. In addition, in cultured hippocampal neurons, reduced expression of N-cadherin by TRAP1 knockdown influences the morphology of dendritic spines. We also report a significant association between several single nucleotide polymorphisms in the *TRAP1* gene and major depression. Our findings indicate that TRAP1 mediates TNF-α/TNF receptor 1 signaling to modulate N-cadherin expression and to regulate cell adhesion and synaptic morphology, which may contribute to the pathogenesis of major depression.

Keywords: cell adhesion, N-cadherin, small interfering RNA, synaptic morphology, tumor necrosis factor receptor, tumor necrosis factor receptor-associated protein 1.

J. Neurochem. (2009) **110**, 496–508.

Received/accepted April 2, 2009.

Address correspondence and reprint requests to Kiyoshi Inoue, Center for Behavioral Neuroscience, Yerkes National Primate Research Center, Emory University School of Medicine, 954 Gatewood Road NE, Atlanta, GA 30322, USA. E-mail: kinoue@emory.edu

[1]These authors contributed equally to this study.

Abbreviations used: DiI, 1,1′-dioctadecyl-3,3,3′,3′-tetramethylindocarbocyanine perchlorate; HSP90, heat shock protein 90; PBS, phosphate buffered saline; siRNA, small interfering RNA; siTRAP1, siRNAs against TRAP1; SNP, single nucleotide polymorphism; STAT, Signal Transducers and Activator of Transcription; TBS, Tris-bufferd saline; TNF, tumor necrosis factor; TNFR, tumor necrosis factor receptor; TRAP1, tumor necrosis factor receptor-associated protein 1.

Tumor necrosis factor-α (TNF-α), which initiates inflammatory immune responses, has been implicated in the pathogenesis of major depression by several lines of evidence (Lanquillon *et al.* 2000; Reichenberg *et al.* 2001; Hestad *et al.* 2003; Jun *et al.* 2003; Tuglu *et al.* 2003; Simen *et al.* 2006; Irwin and Miller 2007). For example, a number of studies have reported that the plasma level of TNF-α is elevated in patients with major depression and can be corrected by anti-depressants in therapy-responders (Lanquillon *et al.* 2000; Hestad *et al.* 2003; Tuglu *et al.* 2003). Infectious and autoimmune diseases are also known to up-regulate serum TNF-α and results in depressive symptoms (Reichenberg *et al.* 2001; Irwin and Miller 2007). Moreover, polymorphisms in the *TNF-α* gene confer susceptibility to major depression (Jun *et al.* 2003). However, little is known about how TNF-α influences neuronal function in the brain.

Tumor necrosis factor-α is a multifunctional cytokine that plays key roles in inflammation, immune response, cell differentiation, proliferation and apoptosis (Pan *et al.* 1997; Baud and Karin 2001). TNF-α is thought to exert its physiological activity through binding to two distinct receptors: type I tumor necrosis factor receptor (TNFR1) and type II tumor necrosis factor receptor (TNFR2). The TNF-α/TNFR1 signaling system has been well documented; it activates several signal transduction pathways including c-*Jun* N-terminal kinase, nuclear factor-κB and caspases (Wallach *et al.* 1999; Baud and Karin 2001; Karin and Lin 2002).

Tumor necrosis factor receptor-associated protein 1 (TRAP1) was initially identified as an interacting protein that binds the intracellular domain of TNFR1 *in vitro* (Song *et al.* 1995). However, the role of TRAP1 in signal transduction through TNFR1 is unknown. TRAP1 is a member of the heat shock protein 90 (HSP90) family and possesses ATPase activity, but lacks chaperone activity (Felts *et al.* 2000). TRAP1 has also been reported to interact with the retinoblastoma protein and tumor suppressors EXT1 and EXT2, but the functional implications of these interactions are unsolved (Chen *et al.* 1996; Simmons *et al.* 1999).

Here we report that TRAP1 works synergistically with TNFR1 to modulate the expression of the cell adhesion molecule N-cadherin, and alters inter-cellular adhesion of neuronal cells. Furthermore, we demonstrate that TRAP1 regulates the morphology of dendritic spines in cultured hippocampal neurons. In addition, we found four single nucleotide polymorphisms (SNPs) changes in the *TRAP1* gene which may predispose patients to major depression.

Materials and methods

In situ hybridization

In situ hybridization was performed as described previously with minor modifications (Furukawa *et al.* 1997). Details are available in the Appendix S1.

Cell culture

Cell cultures were performed as previously described (Kubota *et al.* 2009). Primary hippocampal cultures were prepared from E18 Wistar rat embryos.

Preparation of siRNAs and transfection

Small interfering RNAs (siRNAs) specific to human TRAP1 (si*GENOME SMART* pool siRNA, M-010104-00, GE Healthcare, Buckinghamshire, England), human TNFRSF1A (M-005197-00, GE Healthcare), human TNFRSF1B (M-003934-00, Thermo Fisher Scientific, Waltham, MA, USA) and rat TRAP1 (Accell siRNA, A-08280409, Thermo Fisher Scientific) were purchased. The non-targeting siRNAs for the human genome (si*CONTROL* Non-Targeting siRNA #1, GE Healthcare) or the rat genome (Accell Non-targeting siRNA #1, Thermo Fisher Scientific) were used as a control. siRNA transfection was performed with Lipofectamine RNAiMAX (Invitrogen, Carlsbad, CA, USA) according to the manufacturer's protocol. SH-SY5Y cells were grown to 20–30% confluence in a 3.5 cm dish, transfected with 25 nM or 50 nM siRNA against TRAP1, 50 nM siRNA against TNFR1, TNFR2, or control siRNA, and then incubated for 24, 48 and 72 h. Cultured hippocampal neurons were transfected with 100 nM siRNA specific for TRAP1 mRNA at day 17 *in vitro* (DIV17) and then incubated for 72 h.

Western blot analysis and Immunocytochemistry

Western blot analysis and Immunocytochemistry were done as described (Kubota *et al.* 2009). Antibodies used are listed in the Appendix S1. Cells were fixed with cold methanol for 20 min at −20°C or with 2.5% paraformaldehyde/phosphate buffered saline (PBS) for 20 min for staining of TRAP1 or N-cadherin, respectively. All experiments were performed at least three times.

Cell aggregation assay

The cell aggregation assay was performed as previously described (Takeichi and Nakagawa 2001) with minor modifications. Monolayer cultures of SH-SY5Y cells were prepared by incubating them for 72 h after siRNA transfection. Single cells were harvested in HEPES-buffered Ca^{2+}-, Mg^{2+}-free salt solution (10 mM HEPES-NaOH in Ca^{2+}-and Mg^{2+}-free saline, pH 7.4) containing 0.01% trypsin and 10 mM $CaCl_2$ for 30 min at 37°C. The cells were centrifuged for 3 min at 800 *g* and suspended at 5×10^4 cells/ml in HEPES-buffered Ca^{2+}-, Mg^{2+}-free salt solution containing 1 mM $CaCl_2$. Five hundred μl of cells were added to each well of a bovine serum albumin-coated 24 well tissue culture plate. EGTA was added at 1 mM where indicated. Then the plate was shaken on a gyrating shaker (4630JPN, Barnstead International, Dubuque, IA, USA) for 30 min at 37°C. The aggregation process was examined using a fluorescence microscope (IX71, Olympus, Tokyo, Japan).

Real-time RT-PCR

Forty-eight hours after transfection, total RNA was extracted from the cells using the RNeasy Mini Kit (QIAGEN, Hilden, Germany), and cDNAs were synthesized from 1 μg of total RNA with oligo dT primers using the Omniscript RT kit (QIAGEN). Quantitative RT-PCR was performed using ABI PRISM 7000 (Applied Biosystems, Foster City, CA, USA) according to the manufacturer's instructions. The PCR primers used are as follows:

TRAP1 (NM_016292), 5′-ACCCCAAGGATGTCGGTGA-3′ and 5′-CGGTGCGTCCGTCTTATAGTG-3′;

N-cadherin (NM_001792), 5′-CCCACAGCTCCACCATATG-AC-3′ and 5′-AAGGGAGCTCAAGGACCCAG-3′;

GAPDH (M33197), 5′-CCACTCCTCCACCTTTGACG-3′ and 5′-CACCCTGTTGCTGTAGCCAA-3′;

E2F1 (NM_005225), 5′-TGTAGGACGGTGAGAGCACTTC-3′ and 5′-TTCCCCAGGCTCACCAAAG-3′;

E2F6 (NM_198256), 5′-AGCACCAACGGACCTATCGA-3′ and 5′-TCTCAGATGAAGAGGTCCCGA-3′;

c-Myc (NM_002467), 5′-AAAGGCCCCCAAGGTAGTTATC-3′ and 5′-CGCAACAAGTCCTCTTCAGAAA-3′; and

TNFR1 (NM_001065), 5′-TTCTTGCACAGTGGACCGG-3′ and 5′-CAGAGGCTGCAATTGAAGCAC-3′.

The reaction was first incubated for 2 min at 50°C, then for 10 min at 95°C, followed by 40 cycles of 15 s at 95°C and 1 min at 60°C. Quantitative RT-PCR reactions were performed in triplicate using glyceraldehyde 3-phosphate dehydrogenase (GAPDH) as an internal control.

Luciferase reporter constructs for N-cadherin and E2F1

All PCR products were inserted into the pGL3 (R2.1)-Basic luciferase vector (Promega, Madison, WI, USA). For the N-cadherin-luciferase construct, the promoter region from −1007 to +90, relative to the transcription start site, was cloned by PCR of genomic DNA derived from SH-SY5Y cells. The E2F1-luciferase construct containing the Signal Transducers and Activator of Transcription (STAT) binding site (from −89 to +50) and the ΔSTAT-E2F1-luciferase construct (from −80 to +50) were similarly engineered. The sequences of the forward and reverse primers used are as follows:

N-cadherin, 5′-GGGGTACCTTTCCCGCAGCCCCTCCACCT-3′ and 5′-GAAGATCTAGTTTCCACCCCCTTCCCTTCCCCTCC-3′;

E2F1, 5′-GGGGTACCTTCCCGTCACGGCCGGGGCAG-3′ and 5′-GAAGATCTAGGGCTCGATCCCGCTCCGC-3′; and

ΔSTAT-E2F1, 5′-GGGGTACCCGGCCGGGGCAGCCAATTGT G-3′ and 5′-GAAGATCTAGGGCTCGATCCCGCTCCGC-3′.

Luciferase assays

For knockdown analysis, SH-SY5Y cells plated onto a 3.5 cm dish were transfected with the control phRL-TK construct (0.1 μg, Promega), N-cadherin-luciferase construct (2.5 μg) or E2F1-luciferase construct (2.5 μg) after 36 h of siRNA treatment. For the E2F1 activation assay, SH-SY5Y cells were transfected with the control phRL-TK construct (0.1 μg), N-cadherin-luciferase construct (2 μg), and HA (Hemaglutinin) construct or HA-tagged E2F1 construct (0.4 μg, a gift from Dr M. Imoto). For deletion analysis, the E2F1-luciferase construct (2.5 μg) or ΔSTAT-E2F1-luciferase construct (2.5 μg) with the control phRL-TK construct (0.1 μg) were transfected into SH-SY5Y cells. Transfection of the constructs was performed with Lipofectamine 2000 (Invitrogen) according to the manufacturer's protocol. Twenty-four hours post-transfection, luciferase activities were analyzed by a lumat LB9507 (Berthold Technologies, Bad Wildbad, Germany) using the Promega Dual-Luciferase reporter assay system. All the experiments were performed at least three times in duplicate.

Immunoprecipitation

SH-SY5Y cells were treated with 100 ng/ml TNF-α (Wako, Osaka, Japan) for 15 min at 37°C, harvested in lysis buffer (50 mM HEPES-NaOH, pH 7, 150 mM NaCl, 10% glycerol, 1.2% TritonX-100, 1.5 mM $MgCl_2$, 1 mM EGTA, 1 mM Na_3VO_4, 100 mM NaF and Protease Inhibitor Cocktail EDTA free), incubated for 20 min at 4°C and centrifuged at 17 000 *g* for 20 min at 4°C. Immunoprecipitation was carried out by incubating the supernatant with an anti-TNFR1 antibody (2 μg, Santa Cruz Biotechnology, Santa Cruz, CA, USA) or Negative Control Mouse IgG1 (2 μg, Dako, Glostrup, Denmark) with rotation at 4°C overnight followed by Protein G Sepharose 4 Fast Flow (GE Healthcare) for 2 h at 4°C. The immune complex was rinsed with wash buffer (20 mM HEPES-NaOH, pH 7, 150 mM NaCl, 10% glycerol, 0.1% TritonX-100, 1 mM Na_2VO_3) and boiled with sodium dodecyl sulfate sample buffer for 5 min.

DiI labeling

Cultured hippocampal neurons were grown to day 17 *in vitro* in a 3.5 cm poly-L-lysine–coated glass-bottomed dish (Matsunami Glass, Kishiwada, Japan), transfected with 100 nM siRNA specific to TRAP1 or control siRNA, and then incubated for 72 h. Transfected neurons were fixed with pre-warmed 4% paraformaldehyde for 30 min and washed with PBS. 1,1′-dioctadecyl-3,3,3′,3′-tetramethylindocarbocyanine perchlorate (DiI) (Invitrogen) stock solution (5 mg/ml in dimethylformamide) was diluted to 0.1 mg/ml with cod-liver oil (WAKASA, Osaka, Japan) and centrifuged for 10 min at 17 000 *g*. Each drop of the supernatant was mounted onto the soma of each neuron using FemtoJet and InjectMan NI 2 (Eppendorf, Hamburg, Germany). After 18 h of incubation, DiI labeled neurons were washed with PBS, mounted with Fluoromount (Diagnostic BioSystems, Pleasanton, CA, USA) and analyzed using a confocal laser scanning microscope (LSM-510 UV/META, Carl Zeiss, Oberkochen, Germany).

Statistical analysis

For analysis of the differences between control cells and TRAP1, TNFR1 or TNFR2 knockdown cells in the real-time RT-PCR experiment, luciferase assay, western blotting and morphological analysis of dendritic spines, statistical comparisons were performed using the unpaired Student's *t*-test. Data were considered statistically significant with values of $p < 0.05$ to control.

Genetic analysis

Subjects and methods for genetic analysis are available in the Appendix S1.

Results

TRAP1 is broadly expressed in the CNS exclusively in neurons

Because TRAP1 mRNA has been detected in whole brain lysates (Song *et al.* 1995), we examined the distribution pattern of mRNA and protein in more detail (Figs 1a and S1). *In situ* hybridization revealed that TRAP1 mRNA is broadly expressed throughout the gray matter of the brain and the spinal cord, including the regions known to be

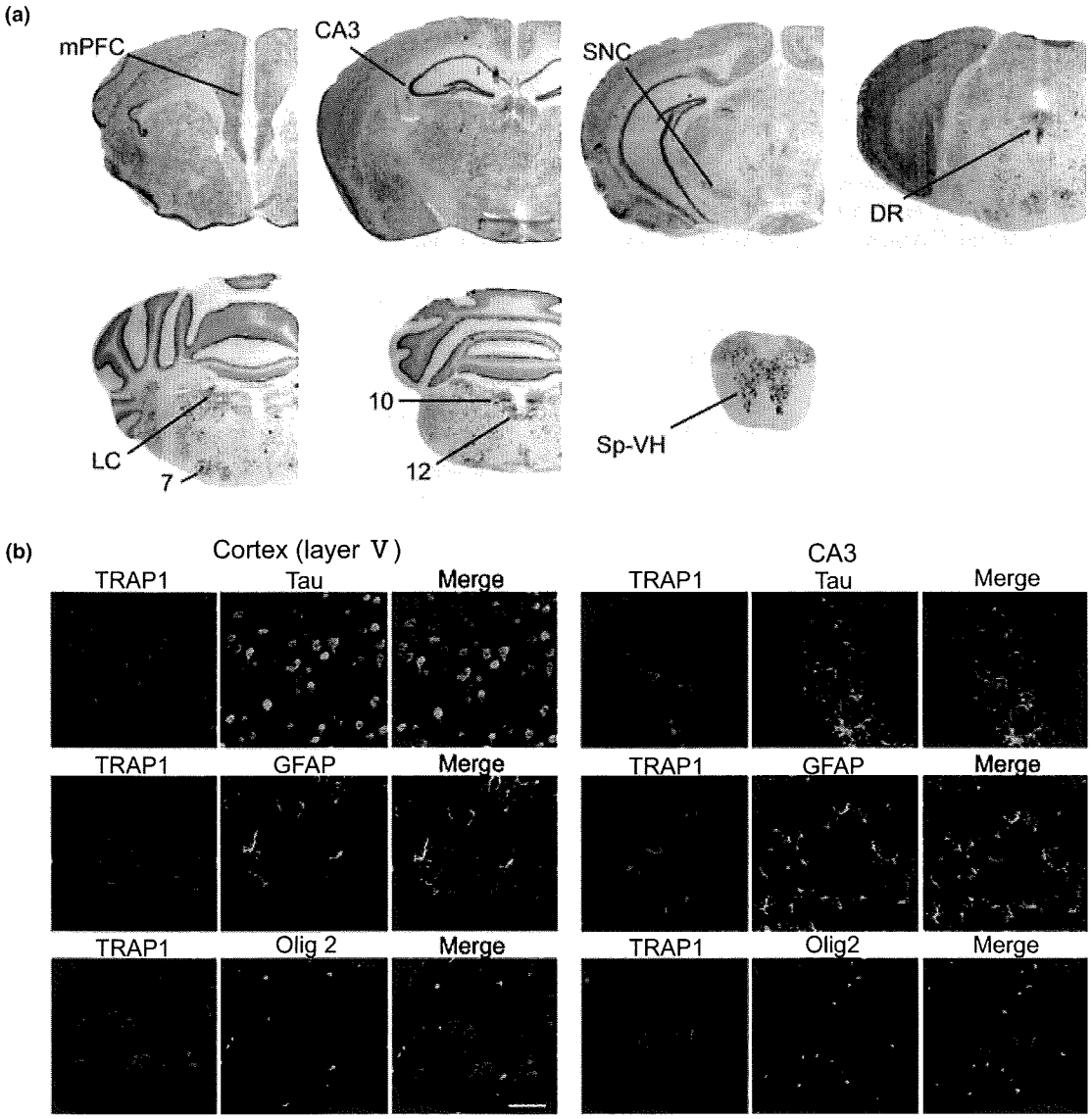

Fig. 1 Distribution of TRAP1 in the mouse brain. (a) *In situ* hybridization of TRAP1 in coronal sections of mouse brain. (b) Double immunostaining of the cortex (left panels) and CA3 of the hippocampus (right panels) with anti-TRAP1 (red), tau (green, top row), GFAP (green, middle row) and olig2 (green, bottom row) antibodies. Scale bar, 50 μm. mPFC, medial prefrontal cortex; CA3, field CA3 of the hippocampus; SNC, substantia nigra pars compacta; DR, dorsal raphe nucleus; LC, locus coeruleus; 7, facial nucleus; 10, the dorsal motor nucleus of the vagus nerve; 12, hypoglossal nucleus; Sp-VH, the ventral horn of the spinal cord; Layer V, layer V of the cortex.

affected in major depression patients, such as the medial prefrontal cortex, the hippocampus and the nuclei producing monoamine: the substantia nigra compacta, dorsal raphe nucleus and locus coeruleus (Nestler *et al.* 2002; Berton and Nestler 2006). Protein localization was also verified by immunostaining with anti-TRAP1 antibody (Fig. S1). Second, because most signals were observed within nuclei of neuron-rich brain regions, we examined whether TRAP1 is expressed predominantly in neurons. TRAP1 expressing cells were co-immunostained with a neuronal marker, tau-1, but not with an astrocyte marker, glial fibrillary acidic protein (GFAP), nor with an oligodendrocyte marker, olig2, in both cortical and hippocampal sections (Fig. 1b). Punctate immunostaining of TRAP1 was detected in the cytoplasm, which is consistent with previously reported mitochondrial localization of TRAP1 in a cell culture (Felts *et al.* 2000).

Cell adhesion is impaired in TRAP1 knockdown cells

To examine the role of TRAP1 in neuronal cells, we used the siRNAs to knockdown TRAP1 in a neuroblastoma cell line, SH-SY5Y. Western blot analysis revealed that siRNAs against TRAP1 (siTRAP1) induced a ~70% decrease of TRAP1 protein compared with that induced by a control siRNA, at 48 h after transfection (Fig. 2a). By immunocytochemistry

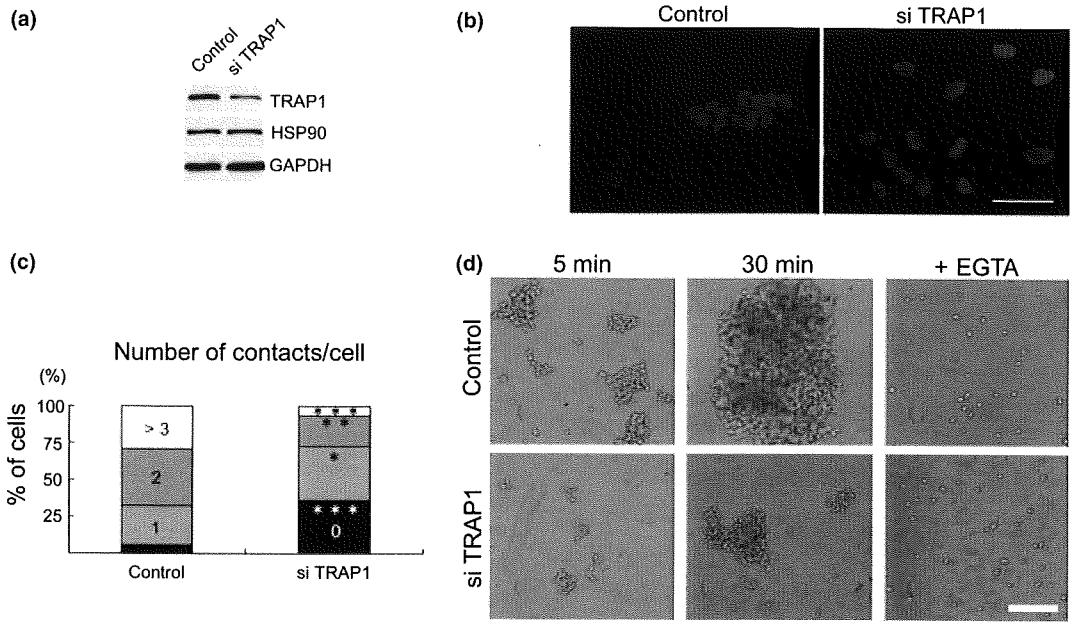

Fig. 2 TRAP1 is involved in cell-cell adhesion. (a) Immunoblotting of SH-SY5Y cells transfected with siRNAs specific to TRAP1 (siTRAP1) or control siRNAs (Control), with anti-TRAP1, HSP90 and GAPDH antibodies. Results are representative of three independent experiments. (b) Immunocytochemistry of TRAP1 knockdown and control cells with anti-TRAP1 antibody (red) and DAPI (blue). Scale bar, 50 μm. (c) Quantification of intercellular adhesion in TRAP1 knockdown cells. Asterisks indicate that the difference is statistically significant. $^{*}p < 0.05$, $^{**}p < 0.01$, $^{***}p < 0.001$ vs. control. (d) Cell-aggregation assay of TRAP1 knockdown cells. Scale bar, 200 μm.

using the same antibody, a ~80% reduction in TRAP1 protein levels by siTRAP1 was observed (Fig. 2b). The siTRAP1 targeted TRAP1 specifically, because levels of HSP90, which has sequence homologous to TRAP1 (Felts *et al.* 2000), was unaffected by the siRNAs (Fig. 2a). Upon knockdown of TRAP1, a striking cell-scattering phenotype was observed in SH-SY5Y cells; cells transfected with siTRAP1 were dispersed throughout the dish, compared to cells transfected with control siRNA that grew in aggregates resembling untransfected SH-SY5Y cells. This phenomenon was detectable as early as 24 h after transfection and became more prominent by 72 h after transfection (Fig. S2a). Immunostaining of actin filaments in the siRNA-treated cells showed no difference in cytoskeletal structure (Fig. S2b). After staining cells for actin, we quantified the percentage of cells with no inter-cellular contacts and detected a 6.2-fold increase in cells transfected with siTRAP1 (36%) compared to cells transfected with control siRNA (5.8%, Fig. 2c). Using the cell aggregation assay, TRAP1 knockdown cells showed much lower efficacy of cell-cell adhesion compared with control cells, suggesting that calcium-dependent cell adhesion is affected (Fig. 2d). These results strongly indicate that TRAP1 regulates downstream molecules crucial for cell adhesion.

N-cadherin is transcriptionally down-regulated in TRAP1 knockdown cells

We further investigated the molecular mechanism responsible for the cell scattering phenotype observed in TRAP1 knockdown cells. Expression levels of cell adhesion molecules, including N-cadherin, are directly related to the cell-scattering phenomenon (Hayashida *et al.* 2006; Yasuda *et al.* 2007) and N-cadherin mediates calcium-dependent cell adhesion in neuronal cells (Takeichi 2007). We therefore determined the expression level of N-cadherin in TRAP1 knockdown cells. We detected that N-cadherin is remarkably decreased throughout the cytoplasm, including around the membrane where cell-adhesion takes place, in the TRAP1 knockdown cells compared to control cells (Fig. 3a). Consistently, immunoblotting experiments showed that expression of N-cadherin is significantly decreased in TRAP1 knockdown cells from as early as 24 h until at least 72 h after transfection, but the expression level of β-catenin, which also regulates cell-adhesion, was unaffected (Fig. 3b). These results suggest that the cell scattering phenotype detected in TRAP1 knockdown cells is at least partially mediated by reduction of N-cadherin expression in those cells.

To determine whether cell viability or migration contributes to the cell-scattering phenotype in TRAP1 knockdown cells, we investigated cell viability by the 3-(4,5-dimethylthiazol-2-yl)-2,5-diphenyltetrazolium bromide (MTT) assay and migration by the wound healing assay (Fig. S2c and d). Although slight decrease of cell viability in TRAP1 knockdown cells was observed compared to the control cells at 48 h after transfection or later, no changes were detected at 24 h after transfection, when the cell-scattering phenotype of

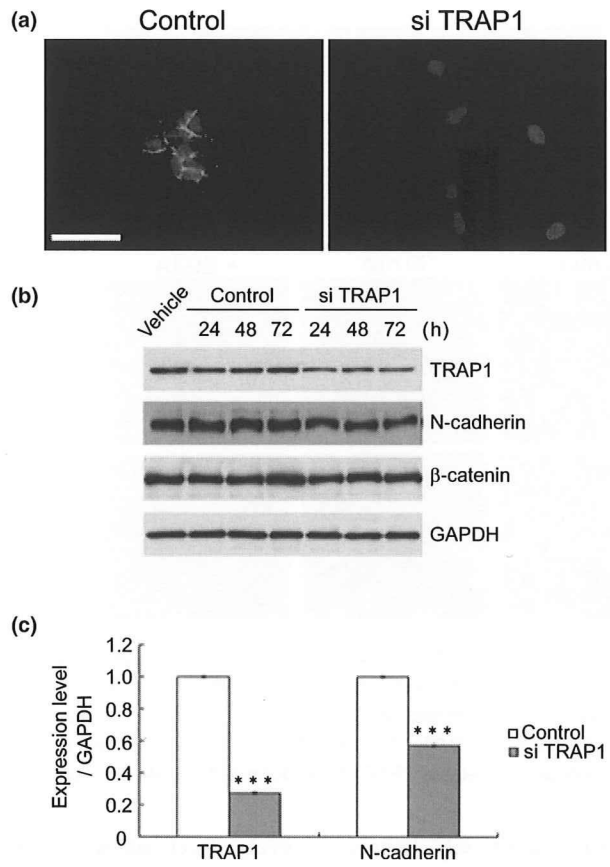

Fig. 3 TRAP1 knockdown results in the down-regulation of N-cadherin. (a) Immunocytochemistry of TRAP1 knockdown cells (right) compared with that of control cells (left) with an anti-N-cadherin antibody (green) and DAPI (blue). Scale bar, 50 μm. (b) Immunoblotting of TRAP1 knockdown cells with anti-TRAP1, N-cadherin, β-catenin and GAPDH antibodies. Results are representative of four independent experiments. (c) Quantitative RT-PCR of TRAP1 and N-cadherin mRNA levels in TRAP1 knockdown cells. GAPDH mRNA was used as an internal control. Data represent the mean ± SD ($n = 3$). ***$p < 0.001$ vs. control.

TRAP1 knockdown cells was already observed (Fig. S2a). No significant changes in the rate of cell migration were observed.

To determine if down-regulation of N-cadherin induced by siTRAP1 occurs at the transcriptional level, we measured levels of N-cadherin mRNA by real-time RT-PCR analysis 48 h after siRNA transfection and found that N-cadherin mRNA in the TRAP1 knockdown cells is about 45% lower than that in the control cells (Fig. 3c). These results indicate that TRAP1 knockdown induces transcriptional down-regulation of N-cadherin.

Taken together, these results suggest that the cell scattering phenotype in the TRAP1 knockdown cells can be mainly attributed to impaired expression of cell adhesion molecules including N-cadherin, which is transcriptionally regulated by TRAP1.

E2F1, a putative transcription factor of N-cadherin, is down-regulated in TRAP1 knockdown cells

To determine if a transcription factor is involved in down-regulation of N-cadherin in TRAP1 knockdown cells, we searched DBTSS (Database of Transcriptional Start Sites) and TRANSFAC (The Transcription Factor Database) and discovered a putative binding site for E2F1 in the promoter region of the N-cadherin gene (Fig. 4a). By immunoblot analysis and real-time PCR, we determined that the amount of both the protein and the mRNA of E2F1 were significantly decreased in TRAP1 knockdown cells (Fig. 4b and c), although the mRNA level of c-Myc, another representative transcription factor, was not affected. Next, we used the luciferase reporter assay to test our hypothesis that E2F1 regulates the expression of N-cadherin. SH-SY5Y cells transfected with the N-cadherin-luciferase plasmid showed strong activity of the reporter, and this activity was suppressed in TRAP1 knockdown cells, mimicking the signal cascade we detected *in vitro* (Fig. 4d). Furthermore, exogenously transfected E2F1 showed a 7.5-fold induction of luciferase reporter activity relative to the control vector (Fig. 4e). These results indicate that E2F1 plays a regulatory role upstream of N-cadherin in the TRAP1 knockdown cells.

Reduced phosphorylation of STAT causes down-regulation of E2F1 in TRAP1 knockdown cells

In search of an upstream molecule that regulates E2F expression, we found a recognition sequence for STAT3 located 89 bp upstream of the transcription initiation site of the E2F1 gene (Fig. 5a). Upon activation, STAT3 proteins are tyrosine-phosphorylated, dimerize and translocate to the nucleus (O'Shea *et al.* 2002). Then the nuclear phospho-STAT3 binds to STAT recognition sites located in the promoter region of downstream genes to promote the transcription of those genes. We detected that the amount of tyrosine-phosphorylated STAT3, but not the total amount of STAT3, was significantly reduced in the TRAP1 knockdown cells (Fig. 5b). Using a reporter construct containing the E2F1 promoter region fused with the luciferase gene, we found that promoter activity of the E2F1 gene was significantly reduced if the STAT3 recognition site was deleted and if TRAP1 was knocked down (Fig. 5c and d). These data indicate that TRAP1 regulates the tyrosine phosphorylation status of STAT3, which controls the expression of E2F, and thus subsequently modulates the transcription of N-cadherin.

Tyrosine phosphorylation of STAT3 and N-cadherin expression are down-regulated in TNFR1 knockdown cells

Tumor necrosis factor receptor-associated protein 1 was originally isolated as a TNFR1 binding protein using the *in vitro* binding assay (Song *et al.* 1995). We confirmed that endogenous TRAP1 was immunoprecipitated with TNFR1 in

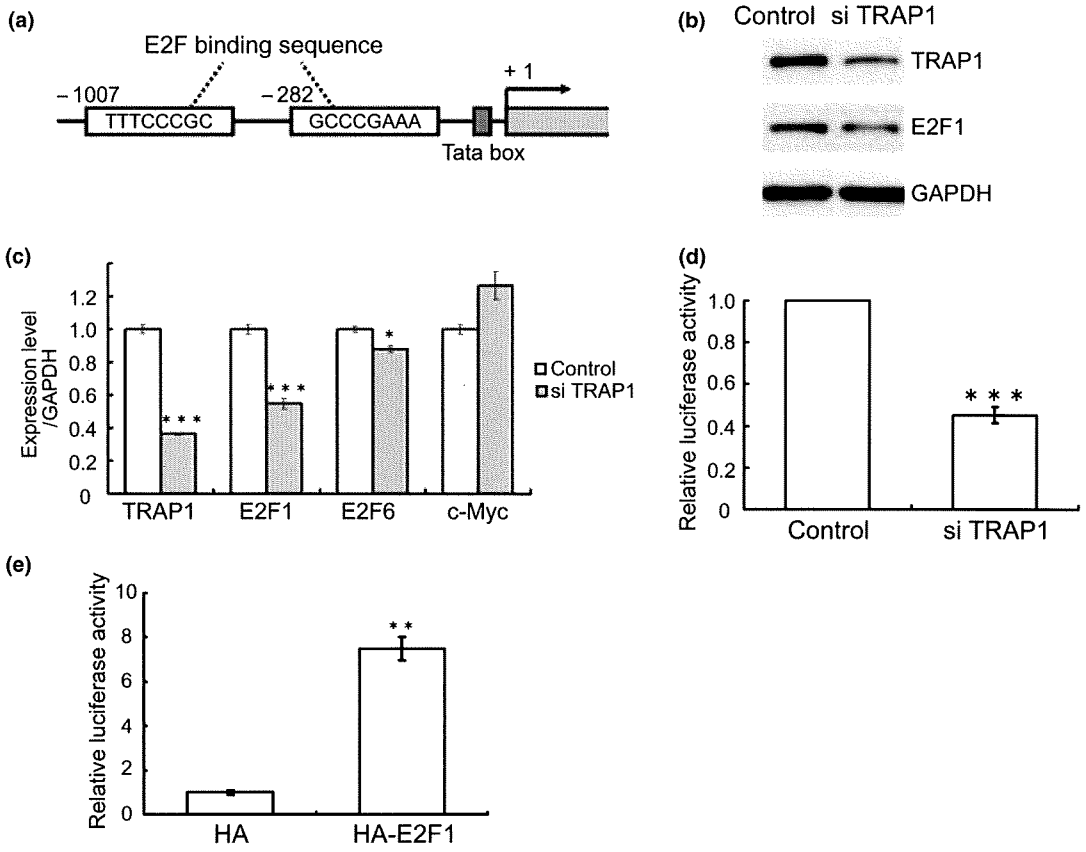

Fig. 4 TRAP1 knockdown decreases transcription activity of the N-cadherin promoter. (a) Schematic illustration of two putative E2F1 binding sequences in the regulatory region of the N-cadherin gene. (b) Immunoblotting of TRAP1 knockdown cells at 48 h after transfection with anti-TRAP1, E2F1 and GAPDH antibodies. Results are representative of three independent experiments. (c) Quantitative RT-PCR of TRAP1, E2F1, E2F6 and c-Myc mRNA levels. GAPDH mRNA was used as an internal control. Data represent the mean ± SD ($n = 3$). (d) Relative transcription activity of the N-cadherin promoter in TRAP1 knockdown cells. (e) Relative transcription activity of the N-cadherin promoter in cells transfected with HA tagged E2F1 (HA-E2F1) compared with that in cells transfected with HA (HA). Data represent the mean ± SD ($n = 3$). $^{*}p < 0.05$, $^{**}p < 0.01$, $^{***}p < 0.001$ vs. control.

SH-SY5Y cells (Fig. 6a). We next investigated whether TRAP1 is functionally associated with TNFR1.

Recently, TNF-α has been reported to activate the Jak-STAT3 pathway through TNFR1 in both peripheral cells and in the brain (Guo *et al.* 1998; Romanatto *et al.* 2007). Given that TRAP1-induced phosphorylation of STAT3 occurs downstream of TNFR1, knockdown of TNFR1 could also lead to a decrease in STAT phosphorylation. We next examined the phosphorylation status of STAT3 in the context of TNFR1 knockdown. An siRNA against TNFR1 (siTNFR1) transfected into SH-SY5Y cells effectively reduced its mRNA level (~78% compared with the control siRNA) and subsequently its protein level (Fig. 6b and c). We detected that the amount of tyrosine-phosphorylated STAT3 was significantly reduced in the TNFR1 knockdown cells (Fig. 6b). Real-time RT-PCR analysis showed decreased mRNA levels of N-cadherin in TNFR1 knockdown cells (Fig. 6c). In addition, we found that exogenous addition of TNF-α for 12 h induced N-cadherin expression (Fig. 6d). This up-regulation was completely blocked if TRAP1 or TNFR1 was knocked down using siRNA, whereas it was not altered in TNFR2 knockdowns (Fig. 6e). Taken together, these results suggest that TRAP1, which binds to the intracellular domain of TNFR1, is involved in the signal transduction pathway from TNFR1 by modulating STAT phosphorylation, resulting in the alteration of N-cadherin expression.

TRAP1 knockdown causes the down-regulation of N-cadherin and alters dendritic spine morphology in cultured hippocampal neurons

We next knocked down TRAP1 using siRNA transfection in cultured hippocampal neurons (Fig. 7a). Because N-cadherin is involved in the morphogenesis of synapses (Togashi *et al.* 2002; Okamura *et al.* 2004), we analyzed whether the morphology of dendritic spines is regulated by TRAP1 via N-cadherin in these neurons (Fig. 7b). According to a standard classification of spine morphology, spines are

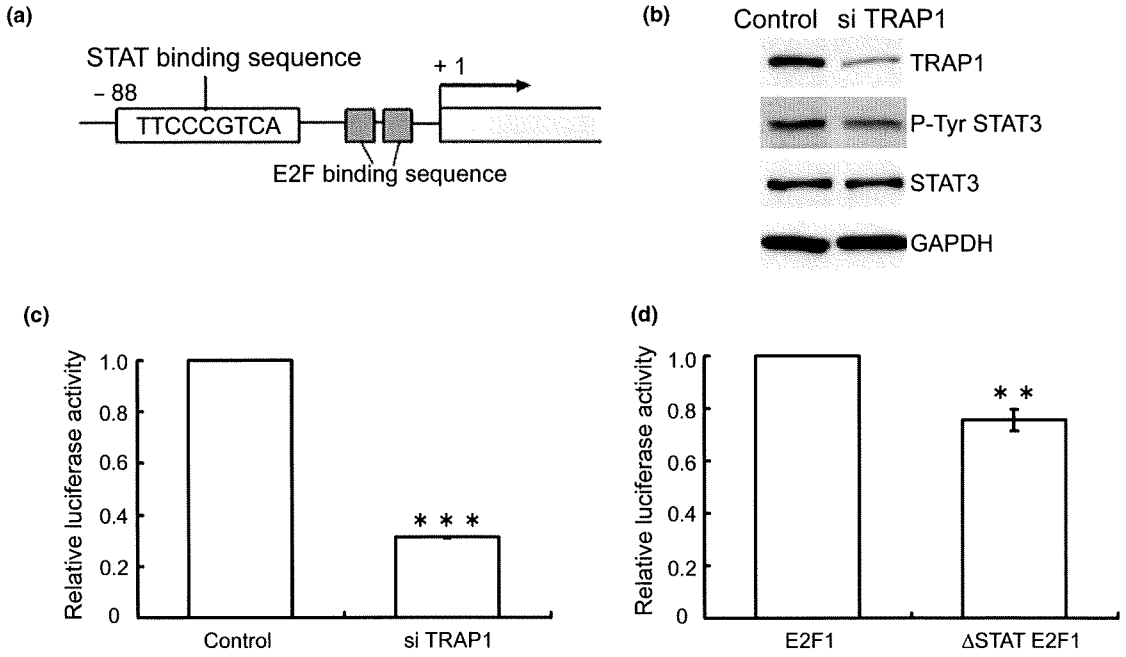

Fig. 5 TRAP1 knockdown decreases transcription activity of the E2F1 promoter. (a) Schematic illustration of a putative STAT binding sequence in the E2F1 promoter region. (b) Immunoblotting of TRAP1 knockdown cells with anti-TRAP1, phosphorylated STAT3 (Tyr705) (p-Tyr STAT3), STAT3 and GAPDH antibodies at 48 h after transfection. Results are representative of three independent experiments. (c) Luciferase assay in TRAP1 knockdown cells transfected with the reporter construct containing the E2F1 promoter. (d) Luciferase assay in TRAP1 knockdown cells transfected with a reporter construct containing the E2F1 promoter (E2F1) or containing E2F1 promoter without STAT3 binding sequence (ΔSTAT E2F1). Data represent the mean ± SD ($n = 3$). $^{**}p < 0.01$, $^{***}p < 0.001$ vs. control.

divided in two types: pedunculated and sessile; the former has a substantial stalk construction whereas the latter does not (Greg *et al.* 1999). In TRAP1 knockdown neurons, spines were predominantly sessile. Only 20.8% of spines displayed peduncular morphology compared with 66.7% in control neurons (Fig. 7c).

Association of SNPs in the *TRAP1* gene with major depression

We then examined the association between SNPs in the *TRAP1* gene and mental disorders, including schizophrenia, bipolar disorder and major depression. Six SNPs in the *TRAP1* gene selected from public databases were genotyped, and the distributions of all six SNPs were verified to be in Hardy-Weinberg proportions in all diagnostic groups (data not shown). As shown in Table 1, a statistically significant association was detected between genetic variations in the *TRAP1* gene and patients with schizophrenia (SNP3, $p = 0.048$), bipolar disorder (SNP1, $p = 0.047$), and major depression (SNP2, $p = 0.003$; SNP3, $p = 0.00086$; SNP4, $p = 0.012$; SNP5, $p = 0.0078$).

Discussion

The primary aim of this study was to elucidate the downstream pathway of TNF-α, whose role is implicated in major depression. Our SNP analyses of the *TRAP1* gene, which binds to the receptor of TNF-α, suggested that the *TRAP1* gene *per se* or another gene in linkage disequilibrium might be associated with psychiatric disorders, particularly with major depression. We showed that TRAP1 is expressed in brain neurons including those in regions closely related to the symptoms of depression (Nestler *et al.* 2002; Berton and Nestler 2006). We further demonstrated that TRAP1 regulates the expression of N-cadherin in the TNF-α/TNFR1 signaling pathway, via regulation of STAT3 tyrosine phosphorylation and E2F expression, resulting in alterations of cell-adhesion efficacy, which causes a morphological change of dendritic spines in cultured hippocampal neurons.

In the CNS, TNF-α is known to be produced by neurons, as well as by astrocytes and microglia (Pan *et al.* 1997). The expression of TNFR1 and TNFR2 in the CNS has also been reported (Bette *et al.* 2003). Although TNFR2 is expressed in non-neuronal cells, TNFR1 is constitutively and broadly expressed in many neurons in the CNS. High levels of TNFR1 expression has been documented in the forebrain regions and in several motor nuclei in the brainstem (Bette *et al.* 2003). Our immunohistochemical analyses showed that the expression pattern of TRAP1 is strikingly similar to that of TNFR1, suggesting that TRAP1 works synergistically with TNFR1 in the brain and contributes to neuronal

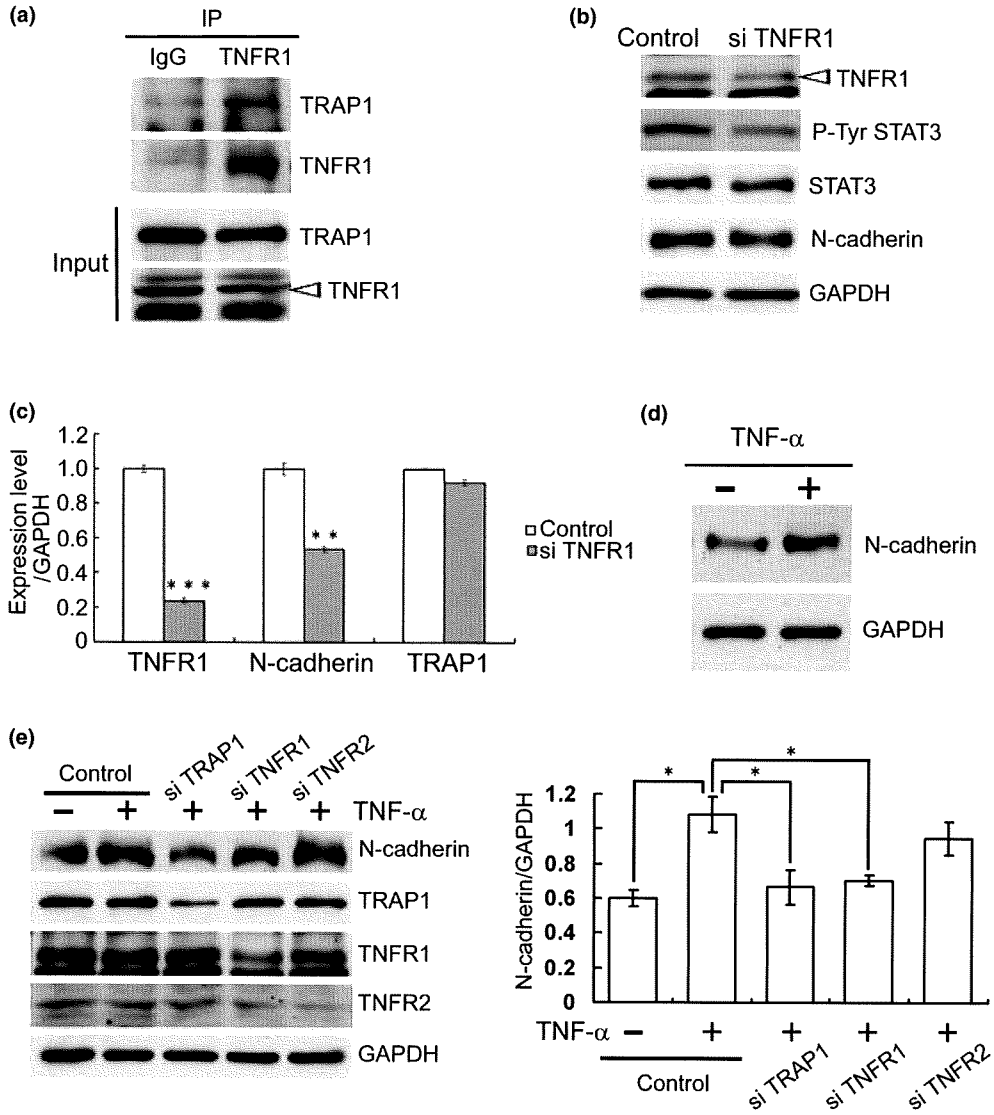

Fig. 6 TRAP1 binds TNFR1 and is involved in N-cadherin expression and phosphorylation of STAT3. (a) Immunoprecipitation of endogenous TNFR1 with endogenous TRAP1 after 15 min of incubation with TNF-α in SH-SY5Y cells. (b) TNFR1 knockdown results in a reduced expression of N-cadherin and tyrosine-phosphorylated STAT3 at 48 h after transfection. (c) Quantitative RT-PCR of TNFR1, N-cadherin and TRAP1 mRNA levels in TNFR1 knockdown. GAPDH mRNA was used as an internal control. (d) TNF-α (100 ng/ml) increases N-cadherin expression at 12 h after treatment. Results are representative of four independent experiments. (e) Knocking down TRAP1 or TNFR1 inhibits N-cadherin up-regulation by TNF-α. GAPDH was used as an internal control. Data represent the mean ± SD ($n = 3$). $^{*}p < 0.05$, $^{**}p < 0.01$, $^{***}p < 0.001$ vs. control.

function. N-cadherin is also expressed in neurons in the adult mouse brain (Redies and Takeichi 1993; Barami *et al.* 1994; Takeichi 2007). Thus, our data verified the co-expression of TNFR1, TRAP1 and N-cadherin in neurons in the brain.

Type I tumor necrosis factor receptor (TNFR1) is localized in the plasma membrane to transmit extracellular TNF-α signals to the intracellular compartment. We have shown that TRAP1 is distributed throughout the cytoplasm including areas near the membrane, and that TRAP1 immunoprecipitates with TNFR1. In addition, we showed that knocking down TNFR1 or TRAP1 has similar effects on N-cadherin expression. Moreover, up-regulation of N-cadherin induced by TNF-α was blocked in TRAP1 or TNFR1 knockdowns. Together, these data indicate that TRAP1 interacts with TNFR1 to modulate cell adhesion.

Considering that mitochondrial TRAP1 undergoes phosphorylation by PINK1 and inhibits cytochrome *c* release from mitochondria (Abeliovich 2007; Pridgeon *et al.* 2007; Mills *et al.* 2008), it is likely that TRAP1 interacts with proteins in various cellular compartments to exert multifaceted functions in the brain, like other members of the HSP90 family (Csermely *et al.* 1998; Pratt 1998).

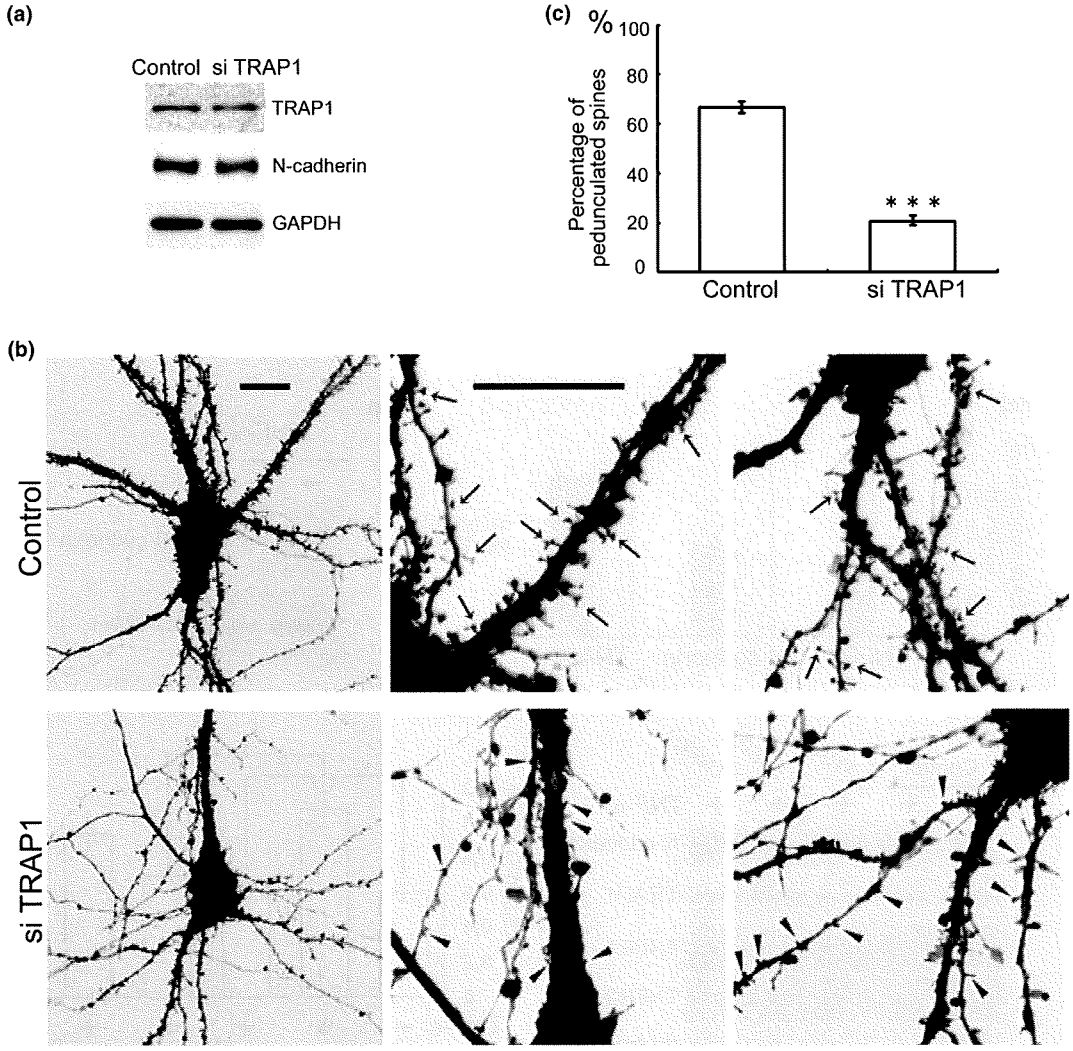

Fig. 7 TRAP1 knockdown alters dendritic morphology in cultured primary hippocampal neurons. (a) Immunoblotting of TRAP1, N-cadherin and GAPDH in TRAP1 knockdown neurons. (b) DiI images of TRAP1 knockdown neurons and control neurons at DIV21. Scale bar, 20 μm. (c) The percentage of pedunculated spines in total spines that are located between 10 and 40 mm from the proximal origin of dendrites in seven each neurons. Data represent the mean ± SD. ***$p < 0.001$ vs. control.

Gene manipulation studies in mice have revealed that a defect in either TNF-α, TNFR1 or cell adhesion molecules has a significantly effects emotional behavior (Manabe *et al.* 2000; Yamada *et al.* 2000; Simen *et al.* 2006). In particular, TNFR1 knockout mice show anti-depression-like behavior (Simen *et al.* 2006). However, little is known about the relationship between TNF-α and cell adhesion molecules in the CNS, although *in vitro* studies in epithelial cells have suggested the involvement of TNF-α in the regulation of cell adhesion molecules (Pober *et al.* 1986; Lassalle *et al.* 1993; Dobbie *et al.* 1999; Young *et al.* 2002). Interestingly, TNF-α-induced over-expression of adhesion molecules has been implicated in the pathogenesis of rheumatoid arthritis, which is frequently accompanied by major depression (Bacon *et al.* 2002; Hurlimann *et al.* 2002; Gonzalez-Juanatey *et al.* 2004). In the present study, we showed that TNF-α up-regulates N-cadherin expression in neuronal cells, thus providing a possible link between TNF-α over-expression and impaired brain functions.

Recent studies have indicated that N-cadherin is an important regulator of synaptic morphology and function (Okamura *et al.* 2004; Tanabe *et al.* 2006; Takeichi 2007). Disrupting N-cadherin in hippocampal neurons with a dominant negative mutant results in altered dendritic spine morphology and aberrant synaptic organization (Togashi *et al.* 2002). Functionally, N-cadherin regulates synaptic plasticity; activity dependent accumulation of N-cadherin at the synapse is essential for spine remodeling and long-term potentiation (Tang *et al.* 1998; Bozdagi *et al.* 2000; Tanaka *et al.* 2000). In addition, activity dependent

Table 1 Allele distributions for six SNPs in the TRAP1 gene among patients with schizophrenia, bipolar disorder and major depression and controls

SNP-ID	dbSNP	Distance from SNP1	Major/ Minor	Location	Cont, $n = 785$	Schizophrenia, $n = 698$			Bipolar disorder, $n = 91$			Major depression, $n = 361$		
							p	OR		p	OR		p	OR
SNP1	rs6500552		T/C	intron1	0.322	0.309	0.45	–	0.396	0.047	1.38	0.328	0.78	–
SNP2	rs1639150	12 189	T/C	intron1	0.45	0.441	0.62	–	0.445	0.91	–	0.384	0.003	0.76
SNP3	rs2108430	21 315	T/C	intron3	0.493	0.529	0.048	1.16	0.527	0.38	–	0.568	0.00086	1.35
SNP4	rs13926	34 928	C/G	exon9 (R307G)	0.496	0.423	0.88	–	0.401	0.52	–	0.482	0.012	1.25
SNP5	rs1136948	37 620	C/G	exon11 (D395E)	0.126	0.107	0.1	–	0.143	0.54	–	0.089	0.0078	0.67
SNP6	rs710891	49 296	T/C	intron16	0.454	0.467	0.48	–	0.429	0.51	–	0.485	0.172	–

Minor allele frequencies in controls are shown. Cont, control; OR, odds ratio.

α-amino-3-hydroxy-5-methylisoxazole-4-propionate (AMPA) receptor trafficking to the synaptic membrane, which is thought to be the molecular basis of learning and memory, is also regulated by N-cadherin (Nuriya and Huganir 2006). These facts indicate that N-cadherin plays important roles in higher brain functions and altered expression of N-cadherin presumably is associated with the pathogenesis of mental disorders. Indeed, N-cadherin is up-regulated in hippocampal neurons by contextual fear conditioning and its dimerization is critical for normal contextual memory formation via the extracellular signal-regulated kinase (ERK) signaling cascade (Schrick *et al.* 2007), also implicated in the pathogenesis of major depression (Dwivedi *et al.* 2001; Coyle and Duman 2003; Einat *et al.* 2003; Hashimoto *et al.* 2006). Our results provide another line of evidence that the signal transduction pathway modulating N-cadherin expression induces morphological changes at synapses, which in turn, plays a key role in cognitive function.

We showed that four SNPs in the *TRAP1* gene may be associated with the pathogenesis of mental disorders, particularly major depression, including two SNPs that cause an amino acid change in the TRAP1 protein: R307G (rs13926) and D395E (rs1136948). Our preliminary study showed that these two non-synonymous SNPs are located in the region critical for the binding of TRAP1 to TNFR1, suggesting that the binding affinity of TRAP1 to TNFR1 or the downstream signaling of TRAP1 might be altered (data not shown). Intronic SNPs have been known to affect alternative splicing, and therefore can be pathogenic (Medina *et al.* 2008; Weickert *et al.* 2008). Functional analysis of SNPs in the *TRAP1* gene, in addition to considering the possibility of linkage disequilibrium is required to clarify the involvement of TRAP1 in the pathogenesis of major depression.

In conclusion, this study provides new and important information towards understanding the causal connections between TNF-α and synaptic function via cell adhesion molecules such as N-cadherin. These findings have important implications for revealing the molecular basis of the pathogenesis of psychiatric disorders, especially major depression, and for future therapeutic interventions for these disorders.

Acknowledgements

The authors thank Dr Masaya Imoto for supplying HA-tagged E2F1, Drs Hidekazu Tanaka, Ko Okamura and Keisuke Sako for technical advice, Drs H Akiko Popiel, Mika Nakamoto and Lisa A. McGraw for critical reading of the manuscript and Akemi Arakawa, Dr Manabu Taniguchi and Yoshihisa Koyama for technical assistance. This study was partly supported by a Grant-in-Aid for Scientific Research from the Ministry of Education, Culture, Sports, Science and Technology of Japan, and a Research Fellowship from the Japan Society for the Promotion of Science for Young Scientists (K.K.).

Supporting Information

Additional Supporting Information may be found in the online version of this article:

Appendix S1 Materials and methods.

Figure S1 Immunohistochemical analysis of TRAP1 in the mouse brain.

Figure S2 (a) Temporal profile of scattered phenotype in TRAP1 knockdown SH-SY5Y cells. Scale bar, 125 μm. (b) Fluorescence images of F-actin in TRAP1 knockdown cells and control cells. Scale bar, 50 μm. (c) Proliferation assay of TRAP1 knockdown cells. (d) Cell migration assay of TRAP1 knockdown cells. Scale bar, 500 μm.

Please note: Wiley-Blackwell are not responsible for the content or functionality of any supporting materials supplied by the authors. Any queries (other than missing material) should be directed to the corresponding author for the article.

References

Abeliovich A. (2007) Parkinson's disease: pro-survival effects of PINK1. *Nature* **448**, 759–760.

Bacon P. A., Stevens R. J., Carruthers D. M., Young S. P. and Kitas G. D. (2002) Accelerated atherogenesis in autoimmune rheumatic diseases. *Autoimmun. Rev.* **1**, 338–347.

Barami K., Kirschenbaum B., Lemmon V. and Goldman S. A. (1994) N-cadherin and Ng-CAM/8D9 are involved serially in the migration of newly generated neurons into the adult songbird brain. *Neuron* **13**, 567–582.

Baud V. and Karin M. (2001) Signal transduction by tumor necrosis factor and its relatives. *Trends Cell Biol.* **11**, 372–377.

Berton O. and Nestler E. J. (2006) New approaches to antidepressant drug discovery: beyond monoamines. *Nat. Rev. Neurosci.* **7**, 137–151.

Bette M., Kaut O., Schafer M. K. and Weihe E. (2003) Constitutive expression of p55TNFR mRNA and mitogen-specific up-regulation of TNF alpha and p75TNFR mRNA in mouse brain. *J. Comp. Neurol.* **465**, 417–430.

Bozdagi O., Shan W., Tanaka H., Benson D. L. and Huntley G. W. (2000) Increasing numbers of synaptic puncta during late-phase LTP: N-cadherin is synthesized, recruited to synaptic sites, and required for potentiation. *Neuron* **28**, 245–259.

Chen C. F., Chen Y., Dai K., Chen P. L., Riley D. J. and Lee W. H. (1996) A new member of the hsp90 family of molecular chaperones interacts with the retinoblastoma protein during mitosis and after heat shock. *Mol. Cell. Biol.* **16**, 4691–4699.

Coyle J. T. and Duman R. S. (2003) Finding the intracellular signaling pathways affected by mood disorder treatments. *Neuron* **38**, 157–160.

Csermely P., Schnaider T., Soti C., Prohaszka Z. and Nardai G. (1998) The 90-kDa molecular chaperone family: structure, function, and clinical applications. A comprehensive review. *Pharmacol. Ther.* **79**, 129–168.

Dobbie M. S., Hurst R. D., Klein N. J. and Surtees R. A. (1999) Upregulation of intercellular adhesion molecule-1 expression on human endothelial cells by tumour necrosis factor-alpha in an in vitro model of the blood-brain barrier. *Brain Res.* **830**, 330–336.

Dwivedi Y., Rizavi H. S., Roberts R. C., Conley R. C., Tamminga C. A. and Pandey G. N. (2001) Reduced activation and expression of ERK1/2 MAP kinase in the post-mortem brain of depressed suicide subjects. *J. Neurochem.* **77**, 916–928.

Einat H., Yuan P., Gould T. D., Li J., Du J., Zhang L., Manji H. K. and Chen G. (2003) The role of the extracellular signal-regulated kinase signaling pathway in mood modulation. *J. Neurosci.* **23**, 7311–7316.

Felts S. J., Owen B. A., Nguyen P., Trepel J., Donner D. B. and Toft D. O. (2000) The hsp90-related protein TRAP1 is a mitochondrial protein with distinct functional properties. *J. Biol. Chem.* **275**, 3305–3312.

Furukawa T., Kozak C. A. and Cepko C. L. (1997) *rax*, a novel paired-type homeobox gene, shows expression in the anterior neural fold and developing retina. *Proc. Natl Acad. Sci. USA* **94**, 3088–3093.

Gonzalez-Juanatey C., Testa A., Garcia-Castelo A., Garcia-Porrua C., Llorca J. and Gonzalez-Gay M. A. (2004) Active but transient improvement of endothelial function in rheumatoid arthritis patients undergoing long-term treatment with anti-tumor necrosis factor alpha antibody. *Arthritis Rheum.* **51**, 447–450.

Greg S., Nelson S. and Michael H. (1999) *Dendrites*. Oxford University Press, New York

Guo D., Dunbar J. D., Yang C. H., Pfeffer L. M. and Donner D. B. (1998) Induction of Jak/STAT signaling by activation of the type 1 TNF receptor. *J. Immunol.* **160**, 2742–2750.

Hashimoto R., Numakawa T., Ohnishi T. *et al.* (2006) Impact of the DISC1 Ser704Cys polymorphism on risk for major depression, brain morphology and ERK signaling. *Hum. Mol. Genet.* **15**, 3024–3033.

Hayashida Y., Urata Y., Muroi E., Kono T., Miyata Y., Nomata K., Kanetake H., Kondo T. and Ihara Y. (2006) Calreticulin represses E-cadherin gene expression in Madin-Darby canine kidney cells via Slug. *J. Biol. Chem.* **281**, 32469–32484.

Hestad K. A., Tonseth S., Stoen C. D., Ueland T. and Aukrust P. (2003) Raised plasma levels of tumor necrosis factor alpha in patients with depression: normalization during electroconvulsive therapy. *J. Ect.* **19**, 183–188.

Hurlimann D., Forster A., Noll G. *et al.* (2002) Anti-tumor necrosis factor-alpha treatment improves endothelial function in patients with rheumatoid arthritis. *Circulation* **106**, 2184–2187.

Irwin M. R. and Miller A. H. (2007) Depressive disorders and immunity: 20 years of progress and discovery. *Brain Behav. Immun.* **21**, 374–383.

Jun T. Y., Pae C. U., Hoon H., Chae J. H., Bahk W. M., Kim K. S. and Serretti A. (2003) Possible association between -G308A tumour necrosis factor-alpha gene polymorphism and major depressive disorder in the Korean population. *Psychiatr. Genet.* **13**, 179–181.

Karin M. and Lin A. (2002) NF-kappaB at the crossroads of life and death. *Nat. Immunol.* **3**, 221–227.

Kubota K., Kumamoto N., Matsuzaki S. *et al.* (2009) Dysbindin engages in c-Jun N-terminal kinase activity and cytoskeletalorganization. *Biochem. Biophys. Res. Commun.* **379**, 191–195.

Lanquillon S., Krieg J. C., Bening-Abu-Shach U. and Vedder H. (2000) Cytokine production and treatment response in major depressive disorder. *Neuropsychopharmacology* **22**, 370–379.

Lassalle P., Gosset P., Delneste Y., Tsicopoulos A., Capron A., Joseph M. and Tonnel A. B. (1993) Modulation of adhesion molecule expression on endothelial cells during the late asthmatic reaction: role of macrophage-derived tumour necrosis factor-alpha. *Clin. Exp. Immunol.* **94**, 105–110.

Manabe T., Togashi H., Uchida N. *et al.* (2000) Loss of cadherin-11 adhesion receptor enhances plastic changes in hippocampal synapses and modifies behavioral responses. *Mol. Cell. Neurosci.* **15**, 534–546.

Medina M. W., Gao F., Ruan W., Rotter J. I. and Krauss R. M. (2008) Alternative splicing of 3-hydroxy-3-methylglutaryl coenzyme A reductase is associated with plasma low-density lipoprotein cholesterol response to simvastatin. *Circulation* **118**, 355–362.

Mills R. D., Sim C. H., Mok S. S., Mulhern T. D., Culvenor J. G. and Cheng H. C. (2008) Biochemical aspects of the neuroprotective mechanism of Pten-induced kinase-1 (Pink1). *J. Neurochem.* **105**, 18–33.

Nestler E. J., Barrot M., DiLeone R. J., Eisch A. J., Gold S. J. and Monteggia L. M. (2002) Neurobiology of depression. *Neuron* **34**, 13–25.

Nuriya M. and Huganir R. L. (2006) Regulation of AMPA receptor trafficking by N-cadherin. *J. Neurochem.* **97**, 652–661.

O'Shea J. J., Gadina M. and Schreiber R. D. (2002) Cytokine signaling in 2002: new surprises in the Jak/Stat pathway. *Cell* **109**(Suppl), S121–S131.

Okamura K., Tanaka H., Yagita Y., Saeki Y., Taguchi A., Hiraoka Y., Zeng L. H., Colman D. R. and Miki N. (2004) Cadherin activity is required for activity-induced spine remodeling. *J. Cell Biol.* **167**, 961–972.

Pan W., Zadina J. E., Harlan R. E., Weber J. T., Banks W. A. and Kastin A. J. (1997) Tumor necrosis factor-alpha: a neuromodulator in the CNS. *Neurosci. Biobehav. Rev.* **21**, 603–613.

Pober J. S., Gimbrone Jr M. A., Lapierre L. A., Mendrick D. L., Fiers W., Rothlein R. and Springer T. A. (1986) Overlapping patterns of activation of human endothelial cells by interleukin 1, tumor necrosis factor, and immune interferon. *J. Immunol.* **137**, 1893–1896.

Pratt W. B. (1998) The hsp90-based chaperone system: involvement in signal transduction from a variety of hormone and growth factor receptors. *Proc. Soc. Exp. Biol. Med.* **217**, 420–434.

Pridgeon J. W., Olzmann J. A., Chin L. S. and Li L. (2007) PINK1 protects against oxidative stress by phosphorylating mitochondrial chaperone TRAP1. *PLoS Biol.* **5**, e172.

Redies C. and Takeichi M. (1993) Expression of N-cadherin mRNA during development of the mouse brain. *Dev. Dyn.* **197**, 26–39.

Reichenberg A., Yirmiya R., Schuld A., Kraus T., Haack M., Morag A. and Pollmacher T. (2001) Cytokine-associated emotional and cognitive disturbances in humans. *Arch. Gen. Psychiatry* **58**, 445–452.

Romanatto T., Cesquini M., Amaral M. E., Roman E. A., Moraes J. C., Torsoni M. A., Cruz-Neto A. P. and Velloso L. A. (2007) TNF-alpha acts in the hypothalamus inhibiting food intake and increasing the respiratory quotient–effects on leptin and insulin signaling pathways. *Peptides* **28**, 1050–1058.

Schrick C., Fischer A., Srivastava D. P., Tronson N. C., Penzes P. and Radulovic J. (2007) N-cadherin regulates cytoskeletally associated IQGAP1/ERK signaling and memory formation. *Neuron* **55**, 786–798.

Simen B. B., Duman C. H., Simen A. A. and Duman R. S. (2006) TNFalpha signaling in depression and anxiety: behavioral consequences of individual receptor targeting. *Biol. Psychiatry* **59**, 775–785.

Simmons A. D., Musy M. M., Lopes C. S., Hwang L. Y., Yang Y. P. and Lovett M. (1999) A direct interaction between EXT proteins and glycosyltransferases is defective in hereditary multiple exostoses. *Hum. Mol. Genet.* **8**, 2155–2164.

Song H. Y., Dunbar J. D., Zhang Y. X., Guo D. and Donner D. B. (1995) Identification of a protein with homology to hsp90 that binds the type 1 tumor necrosis factor receptor. *J. Biol. Chem.* **270**, 3574–3581.

Takeichi M. (2007) The cadherin superfamily in neuronal connections and interactions. *Nat. Rev. Neurosci.* **8**, 11–20.

Takeichi M. and Nakagawa S. (2001) Cadherin-dependent cell-cell adhesion. *Curr. Protoc. Cell Biol.* Chapter 9, Unit 9.3.

Tanabe K., Takahashi Y., Sato Y., Kawakami K., Takeichi M. and Nakagawa S. (2006) Cadherin is required for dendritic morphogenesis and synaptic terminal organization of retinal horizontal cells. *Development* **133**, 4085–4096.

Tanaka H., Shan W., Phillips G. R., Arndt K., Bozdagi O., Shapiro L., Huntley G. W., Benson D. L. and Colman D. R. (2000) Molecular modification of N-cadherin in response to synaptic activity. *Neuron* **25**, 93–107.

Tang L., Hung C. P. and Schuman E. M. (1998) A role for the cadherin family of cell adhesion molecules in hippocampal long-term potentiation. *Neuron* **20**, 1165–1175.

Togashi H., Abe K., Mizoguchi A., Takaoka K., Chisaka O. and Takeichi M. (2002) Cadherin regulates dendritic spine morphogenesis. *Neuron* **35**, 77–89.

Tuglu C., Kara S. H., Caliyurt O., Vardar E. and Abay E. (2003) Increased serum tumor necrosis factor-alpha levels and treatment response in major depressive disorder. *Psychopharmacology (Berl)* **170**, 429–433.

Wallach D., Varfolomeev E. E., Malinin N. L., Goltsev Y. V., Kovalenko A. V. and Boldin M. P. (1999) Tumor necrosis factor receptor and Fas signaling mechanisms. *Annu. Rev. Immunol.* **17**, 331–367.

Weickert C. S., Miranda-Angulo A. L., Wong J., Perlman W. R., Ward S. E., Radhakrishna V., Straub R. E., Weinberger D. R. and Kleinman J. E. (2008) Variants in the estrogen receptor alpha gene and its mRNA contribute to risk for schizophrenia. *Hum. Mol. Genet.* **17**, 2293–2309.

Yamada K., Iida R., Miyamoto Y., Saito K., Sekikawa K., Seishima M. and Nabeshima T. (2000) Neurobehavioral alterations in mice with a targeted deletion of the tumor necrosis factor-alpha gene: implications for emotional behavior. *J. Neuroimmunol.* **111**, 131–138.

Yasuda S., Tanaka H., Sugiura H. *et al.* (2007) Activity-induced protocadherin arcadlin regulates dendritic spine number by triggering N-cadherin endocytosis via TAO2beta and p38 MAP kinases. *Neuron* **56**, 456–471.

Young J. L., Libby P. and Schonbeck U. (2002) Cytokines in the pathogenesis of atherosclerosis. *Thromb. Haemost.* **88**, 554–567.

Schizophrenia Research 108 (2009) 93–103

Contents lists available at ScienceDirect

Schizophrenia Research

journal homepage: www.elsevier.com/locate/schres

Impaired regional hemodynamic response in schizophrenia during multiple prefrontal activation tasks: A two-channel near-infrared spectroscopy study

Koji Ikezawa [a,*], Masao Iwase [a], Ryouhei Ishii [a], Michiyo Azechi [a], Leonides Canuet [a], Kazutaka Ohi [a], Yuka Yasuda [a,b,1], Naomi Iike [a], Ryu Kurimoto [a], Hidetoshi Takahashi [a], Takayuki Nakahachi [a], Ryuji Sekiyama [c,2], Tetsuhiko Yoshida [c,2], Hiroaki Kazui [a], Ryota Hashimoto [a,b,d,1], Masatoshi Takeda [a]

[a] Department of Psychiatry, Osaka University Graduate School of Medicine, D3, 2-2 Yamadaoka, Suita, Osaka, 565-0871 Japan
[b] The Osaka-Hamamatsu Joint Research Center for Child Mental Development, Osaka University Graduate School of Medicine, D3, 2-2 Yamadaoka, Suita, Osaka, 565-0871 Japan
[c] Department of Neuropsychiatry, Osaka National Hospital, 2-1-14 Houenzaka, Tyuou-ku, Osaka, Osaka, 540-0006 Japan
[d] CREST (Core Research for Evolutionary Science and Technology), JST (Japan Science and Technology Agency), Kawaguchi, Saitama, Japan

ARTICLE INFO

Article history:
Received 5 June 2008
Received in revised form 1 December 2008
Accepted 4 December 2008
Available online 20 January 2009

Keywords:
Schizophrenia
Near-infrared spectroscopy (NIRS)
Frontal lobe dysfunction
Physiological marker

ABSTRACT

In schizophrenia, dysfunction of the prefrontal cortex (PFC), regarded as a core feature of the disease, has been investigated by different neuroimaging methods. Near infrared spectroscopy (NIRS), a novel neurophysiological method, is being increasingly used in the investigation of frontal dysfunction in schizophrenia. However, NIRS measurements during multiple frontal activation tasks have been rarely reported. The purpose of this study was to compare hemodynamic changes in the PFC between patients with schizophrenia and healthy controls during four different types of frontal lobe tasks using a 2-channel NIRS system. Thirty patients with schizophrenia and thirty age- and gender-matched healthy controls were enrolled in this study. In both groups, changes in oxygenated hemoglobin concentration (Δ[oxyHb]) at the bilateral forehead were measured during Verbal fluency test letter version (VFT-letter), VFT category version, Tower of Hanoi (TOH), the Sternberg and Stroop tasks. Regarding Δ[oxyHb] in PFC, a diagnosis group effect was found for VFT-letter and TOH. Significant negative correlation was found between left Δ[oxyHb] during TOH and negative and cognitive symptom scores in schizophrenia patients. Right Δ[oxyHb] during TOH also showed significant negative correlation with cognitive symptoms scores. No significant correlation between Δ[oxyHb] and clinical characteristics were observed during VFT-letter. These findings suggest that among a battery of frontal lobe tasks administered to schizophrenia patients, VFT-letter and TOH are more sensitive to detect PFC activation, as indicated by Δ[oxyHb] using a 2-channel NIRS. Taken together, these findings and those of previous neuroimaging studies suggest that VFT-letter and TOH might represent possible candidate physiological markers of prefrontal dysfunction in schizophrenia, though extensive testing in clinical settings will be necessary.

1. Introduction

Schizophrenia is a mental disorder emerging in adolescence that is typically characterized by hallucinations and delusions as well as emotional and social dysfunction. Recently, marked cognitive impairments, predominantly in memory, attention, and executive functions have been described in patients with

* Corresponding author. Tel.: +81 6 6879 3051; fax: +81 6 6879 3059.
E-mail address: ikezawa@psy.med.osaka-u.ac.jp (K. Ikezawa).
[1] Tel.: +81 6 6879 3074; fax: +81 6 6879 3059.
[2] Tel.: +81 6 6942 1331; fax: +81 6 6943 6467.

0920-9964/$ – see front matter © 2008 Elsevier B.V. All rights reserved.
doi:10.1016/j.schres.2008.12.010

schizophrenia and are regarded as being independent of psychiatric symptoms (Heinrichs and Zakzanis, 1998). In fact, cognitive impairments in multiple domains are considered important features of the psychopathology of schizophrenia and have been reported in association with social functions, quality of life, and prognosis of social life (Harvey et al., 1998). These cognitive impairments are related to dysfunction of several areas in the brain in schizophrenia including the prefrontal area. Previous studies on schizophrenia have reported poor performance of neuropsychological tests that assess prefrontal function such as the Verbal Fluency Test (VFT), the Wisconsin Card Sorting Test (WCST – measuring conversion of the concept and flexibility of reaction), and the Stroop task (measuring attention and inhibition, see Ma et al., 2007). Several functional MRI (fMRI) studies indicated involvement of the prefrontal cortex (PFC) in the WCST in healthy controls (Alvarez and Emory, 2006), and decreased activation of the PFC in schizophrenia (Ragland et al., 2007). Assessing prefrontal function is therefore essential to elucidate the schizophrenia pathophysiology.

Near-infrared spectroscopy (NIRS), a novel neuroimaging method, is increasingly used in investigating psychiatric disorders. This method exploits the property of near-infrared light penetrating into tissues where it is absorbed by hemoglobin depending on the oxygenation state of the hemoglobin (Jobsis, 1977). Using different infrared wavelengths, it is thus possible to measure relative changes in oxygenated hemoglobin concentration ([oxyHb]) and deoxygenated hemoglobin ([deoxyHb], Hoshi, 2003; Soul and du Plessis, 1999). It is well established that oxygen consumption, regional cerebral blood response (rCBR), and oxygenated hemoglobin supply are increased in the highly activated neural regions (Hoshi et al., 2001; Fox and Raichle, 1986).

Compared to other neuroimaging methods such as fMRI and PET, NIRS measurement is quite simple, which is advantageous in a clinical setting. NIRS is non-invasive in nature, portable, has a low running cost and it is available for continuous and repetitive measurements, albeit with the limitation of low spatial resolution and the inability to examine deep brain structures. Since several studies have successfully utilized NIRS in various psychiatric disorders such as schizophrenia, bipolar disorder, and dementia (Richter et al., 2007; Kameyama et al., 2006; Suto et al., 2004; Fallgatter et al., 1997), there are growing expectations for clinical NIRS applications in the neuropsychiatric area.

Several NIRS studies have reported a significantly smaller increase in [oxyHb] in the PFC in schizophrenia during execution of frontal lobe tasks like the VFT or the Random Number Generation Task (Takizawa et al., 2008; Ehlis et al., 2008; Hoshi et al., 2006; Folley and Park, 2005; Kubota et al., 2005; Watanabe and Kato, 2004; Shinba et al., 2004; Suto et al., 2004; Fallgatter and Strik, 2000; Okada et al., 1994). However, only few frontal lobe tasks have been assessed in these studies, and a comprehensive look at PFC activity is not available. To address this, we employed a 2-channel NIRS (2ch-NIRS) system and four kinds of cognitive tasks (VFT, Tower of Hanoi or TOH, the Sternberg, and the Stroop) to examine which tasks were suitable for finding significant differences in task-induced changes in [oxyHb], and for showing association between the changes in rCBR and demographic and clinical parameters in schizophrenia. VFT, TOH, the Sternberg and the Stroop tasks measure fluency, executive function, working memory, and attention/inhibition, respectively (Ma et al., 2007; Johnson et al., 2006), and they are generally regarded as representative neuropsychological tasks to elicit PFC activation (Ragland et al., 2007; Alvarez and Emory, 2006; Fincham et al., 2002, Schlösser et al., 2008; Johnson et al., 2006). Using 2ch-NIRS to measure changes in rCBR during these tasks is relatively simple and readily adoptable for clinical purposes.

Unlike previous studies with multi-channel NIRS, in this study, changes in [oxyHb] were measured at the bilateral forehead overlying the PFC using a 2ch-NIRS system. Despite it having only two channels, there are several advantages to the 2ch-NIRS system. For instance, invalid NIRS data from a low signal/noise ratio common to multi-channel systems on haired scalp (Suto et al., 2004) is not a problem for NIRS measurements on the forehead. In addition, preparations for 2ch-NIRS measurements take only few seconds, while several minutes are needed for the placement of the probes with multi-channel systems. Furthermore, identical cross-subject anatomical positioning in 2ch-NIRS is supported by fixing the probes at Fp1-F7 and Fp2-F8 according to the 10/20 international electrode placement system for electroencephalography; similar anatomical channel positioning is difficult in multi-channel systems due to variations in head size. Subjects also feel considerable pain at the scalp with multi-channel systems, but not with 2ch-NIRS, which may improve the quality of the PFC recording. Finally, 2-channel data acquisition has no need for statistical corrections for multiple comparisons as does multi-channel data acquisition (Nakahachi et al., 2008).

The purpose of this study was to compare changes in rCBR in the PFC between schizophrenia and healthy controls, and to investigate potential association between changes in rCBR and demographic and clinical parameters in schizophrenia using four frontal lobe tasks and simple, non-invasive 2ch-NIRS measurements. Based on previous reports indicating an association between hypofrontality and negative symptoms in schizophrenia (Pratt et al., 2008; Semkovska et al., 2001), we hypothesized that PFC activation during these tasks in schizophrenia patients would be less than that of healthy controls. We also anticipated a significant correlation between the magnitude of PFC activation and clinical parameters in schizophrenia patients.

2. Methods

2.1. Subjects

This study was conducted with 30 schizophrenia patients and 30 age/gender-matched healthy controls. All patients with schizophrenia were diagnosed according to the Structured Clinical Interview of the Diagnostic and Statistical Manual of Mental Disorders, 4th Edition (DSM-IV; American Psychiatric Association, 1994). They were treated as inpatients or outpatients at the Department of Psychiatry, Osaka University Hospital from November 2006 to April 2007. Psychopathology was assessed using the Positive and Negative Syndrome Scale (PANSS; Kay et al., 1987) and summarized using the five-factor model of PANSS (Lindenmayer et al., 1994). Antipsychotic medication-related extrapyramidal

symptoms were assessed using the Drug-Induced Extrapyramidal Symptom Scale (DIEPSS; Inada, 1996). Control subjects were not taking any medications at the time of recruitment and had no personal or family history of psychiatric and/or neurological disorders. All subjects were right-handed as indicated by the Edinburgh Handedness Inventory (Oldfield, 1971). Their premorbid IQs were assessed using the Japanese version of the National Adult Reading Test (JART; Matsuoka et al., 2006). This study was approved by the Ethics Committee of Osaka University, and written informed consent was obtained from all subjects prior to the experiments. All procedures were carried out in accordance with the policies and principles contained in the Declaration of Helsinki. The demographic and clinical characteristics of all subjects are shown in Table 1.

2.2. Tasks and procedure

All subjects sat on a comfortable chair in a silent room. The tasks comprised pre-task (30 s), task and post-task periods (60 s). The durations of the task period of VFT-letter, VFT-category and TOH was 60 s, while the Sternberg and the Stroop tasks had durations of 120 s. Because most previous NIRS studies which applied VFT used a 60-sec task period, we allocated the same period of time to VFT in this study. As for TOH, a 60-sec task period proved to elicit sufficient cortical activation in our preliminary measurements. However, the task period for the Sternberg and the Stroop tasks were set at 120 s based on preliminary findings indicating that 60 s was insufficient for significant activation.

Table 1
Demographic data and clinical characteristics

	Schizophrenia (30)	Healthy controls (30)
Age	38.7±11.7	37.3±8.7
Sex (M/F)	12/18	13/17
Years of education	13.3±2.4**	15.5±2.1
JART	101.2±10.8	105.9±8.4
Onset age	23.4±8.4	
Duration of illness (year)	14.7±13.0	
Duration of antipsychotic medication (year)	11.9±12.5	
Equivalents of CPZ (mg)	842.6±704.2	
Equivalents of BZD (mg)	17.1±11.1 [a]	
Admission (time)	3.0±3.7	
Duration of admission (month)	15.0±41.5	
PANSS		
Positive symptoms	18.8±5.5	
Negative symptoms	18.2±6.4	
General psychopathology	36.8±9.1	
Five-factor model of PANSS		
Positive	15.7±5.3	
Negative	16.7±6.5	
Cognitive	10.9±4.0	
Excitement	6.7±2.5	
Depression/anxiety	9.2±3.0	
DIEPSS	2.5±2.9	

Data are presented as mean±SD. JART, the Japanese version of the National Adult Reading Test; CPZ, chlorpromazine; BZD, benzodiazepines; PANSS, the Positive and Negative Syndrome Scale; DIEPSS, the Drug-Induced Extrapyramidal Symptom Scale.
**$p<0.01$, Mann–Whitney U test was used.
[a] Eleven patients were taking BZD medications.

The VFT-letter version asks the subjects to generate loudly as many nouns as possible, all of which start with the Japanese *hiragana* letters 'a', 'ka', and 'sa', with a duration of 20 s for each letter. The VFT-category version asks the subjects to generate loudly as many nouns as possible related to three different categories: animals, vegetables, and vehicles, with a 20-sec duration for each category. In both tasks, the subjects were asked to pronounce the vowels 'a', 'i', 'u', 'e', 'o' repeatedly during the pre- and post-task periods. These tasks evaluate the ease with which a person can produce words. The total number of generated words was deemed task performance. The generated words during the measurement were written down by testers immediately. This procedure is explained in detail elsewhere (Kubota et al., 2005).

The TOH consists of three pegs of equal size and a number of disks of different sizes which can slide onto any peg. The subjects were instructed to follow three rules to perform the task. First, only one disk may be moved at a time. Second, no disk may be place on top of a smaller disk. Third, at no time may a disk be put in a place other than a peg. Upon following these rules, the subjects were asked to transfer the disks, which were neatly piled up in order of size on one peg, to another peg to form the original conical shape in as few moves as possible. To remove non-specific activation elicited by hand motion, they were instructed to move the smallest disk slowly and continuously during the pre- and post-task periods. Before the measurements, the subjects were asked to perform the task with three disks to confirm that they understood the instructions. In TOH with four disks, the fewest moves to achieve the goal is 15. The total number of effective moves was deemed task performance. If the subjects completed the task within 60 s, they were asked to repeat the task. In this case, the total number of effective moves was deemed task performance. The total number of moves and total number of effective moves during measurement were written down by testers immediately. For details on the procedure see Giménez et al. (2003).

In the Sternberg and the Stroop tasks, digits and characters, respectively, were displayed on a 15-inch monitor connected to a desktop PC placed approximately 1 meter away from the subjects. These tasks were performed using the Multi Trigger System version 2.10 (MedicalTrySystem, Japan). The Sternberg task consisted of a modified version of the Sternberg Item Recognition Paradigm (Sternberg, 1966), which has two phases, namely the encoding phase and the probe phase. During the encoding phase, five random digits were displayed one by one for 2 s. Following an eye fixation mark (cross mark) for 3 s, a probe digit was displayed for 1 s with an inter-stimulus interval (ISI) of 2 s and the probe presentation was repeated three times during the probe phase. For each probe, subjects were asked to recognize whether a probe digit was included or not in the random digits displayed during the encoding phase. For each question, they answered quickly "yes" or "no", as appropriate. The eye fixation mark was displayed for 3 s between each set of digits. The total number of sets was eight. Each random five digits and each combination with a probe digit were different among the eight sets. The presentation was the same for all subjects. The subjects were asked to watch the eye fixation mark during the pre- and post-task periods. They performed practice trials prior to the measurements to allow them to

understand the task's components. The total number of correct answers was deemed task performance. The full performance was 24. The answers during the measurement were written down by testers immediately. For details on the procedure see Casement et al. (2006).

During the Stroop task, each name of four colors (blue, yellow, red, green), written in Japanese *kanji* character, was presented in congruent (e.g., the word BLUE displayed in blue color) or incongruent combinations (e.g., the word YELLOW displayed in red color). This task consisted of twelve

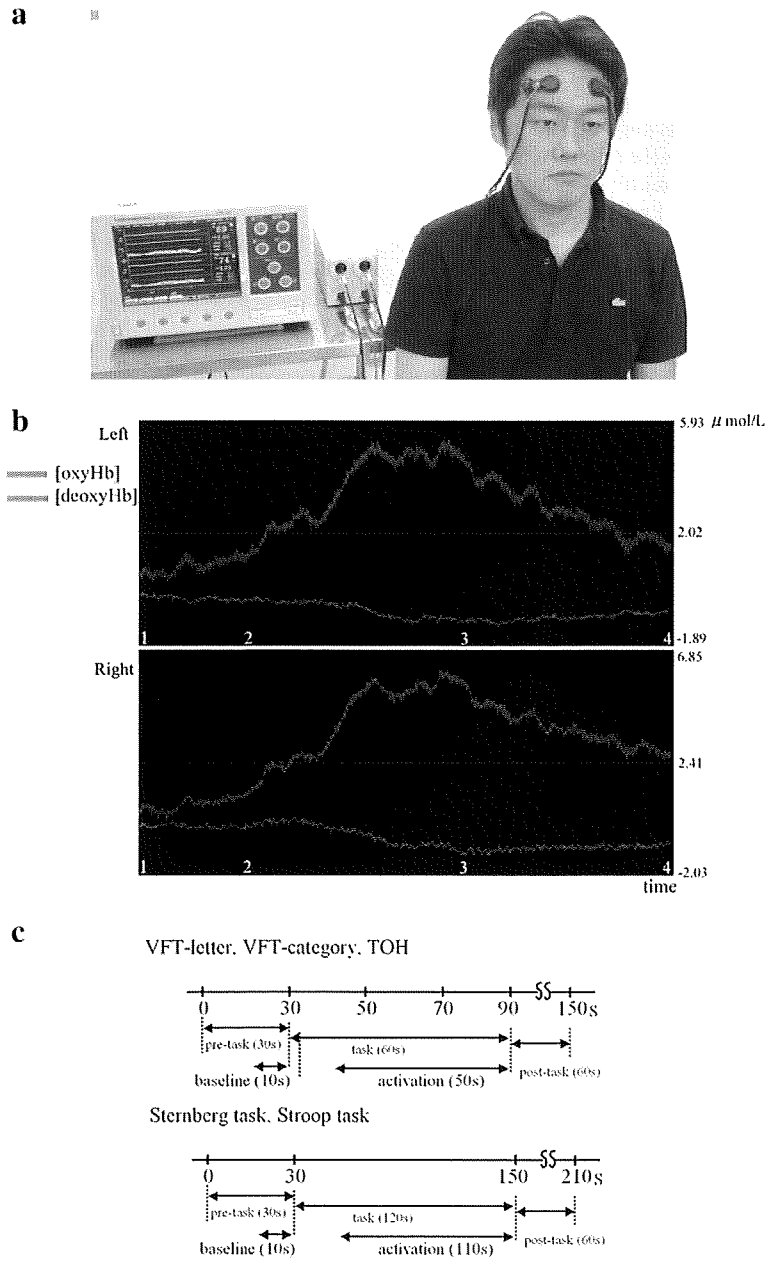

Fig. 1. a. The 2-channel NIRS measurements and the probe setting. b. Actual NIRS data along time course during TOH in one representative healthy control. Upper row shows measurement at left forehead, lower row shows measurement at right forehead. Red line means [oxyHb], blue line means [deoxyHb]. In figure, "1" means the beginning of pre-task, "2" means the beginning of task, "3" means the end of task (also the beginning of post-task), "4" means the end of post task. c. Protocols and procedures of data analysis in each task. Pre-task and post-task periods for all tasks had durations of 30 s and 60 s, respectively. The durations of the task periods of VFT-letter, VFT-category and TOH were 60 s, and those of the Sternberg and the Stroop tasks were 120 s. In data analysis, the mean levels of [oxyHb] ([deoxyHb]) during the last 10 s of the pre-task period were defined as baseline. The mean levels of [oxyHb] ([deoxyHb]) during the last 50 s task period of VFT-letter, VFT-category, and TOH were defined as activation levels. The mean levels of [oxyHb] ([deoxyHb]) during the last 110 s task period of the Sternberg task and the Stroop task were defined as activation levels. The difference between activation and baseline levels was deemed size of activation (Δ[oxyHb], Δ[deoxyHb]). VFT-letter, Verbal Fluency Test-letter; VFT-category, Verbal Fluency Test-category; TOH, Tower of Hanoi. (For interpretation of the references to color in this figure legend, the reader is referred to the web version of this article.)

congruent and twelve incongruent trials. The colored characters were presented for 1.25 s with an ISI of 1.75 s. Each trial was presented consecutively in a random order to avoid habituation. For each trial, the subjects were asked to orally identify the color of each printed color name, but not the color name displayed on the screen, as quickly as possible. An eye fixation mark was also used during the pre- and post-task periods of this task, and all subjects performed practice trials as well. The total number of correct answers was deemed task performance. The full performance was 40. The answers during the measurement were written down by testers immediately. This procedure is explained in detail elsewhere (Kawaguchi et al., 2005). To address the potential order effect, the order of these tasks was divided into the two following patterns, which were applied to each subject alternately: order A) VFT-letter → VFT-category → TOH → Sternberg task → Stroop task, order B) Stroop task → Sternberg task → TOH → VFT-category → VFT-letter.

2.3. NIRS measurements

NIRS measurements were carried out with a 2-channel system (NIRO-200, Hamamatsu Photonics, Japan). The NIRO-200 utilizes near-infrared light emitted at three different wavelengths (775, 810, and 850 nm) to detect primal changes in [oxyHb] and [deoxyHb] of venous blood in brain cortical regions. Two pairs of emission (light source: laser-diode) and detection probes (light detector: photo-diode) were attached to the bilateral forehead of the subjects. One detection probe was located at Fp1 and the corresponding emission probe at F7, while the other pair of probes was located at Fp2-F8, according to the international 10/20 electrode placement system for electroencephalography (see Fig. 1-a). The distance between the detection probe and the corresponding emission probe was 3 cm. These probe settings enabled us to detect hemodynamic changes in two separate cortical areas. The anatomical location of these areas likely corresponded to part of the superior and inferior frontal gyri (Okamoto et al., 2004). The two sets of probes do not interfere with each other for simultaneous recording of [oxyHb] or [deoxyHb] changes. Recordings were acquired at a sampling rate of 6 Hz. The estimated path length factor was 24 cm. All hemoglobin oxygen concentration values are expressed in μmol/L. Actual NIRS data along time course is shown in Fig. 1-b.

2.4. Statistical analysis

Since [oxyHb] is a more sensitive indicator of changes in rCBR compared to [deoxyHb] (Hoshi et al., 2001; Hoshi, 2003), changes in [oxyHb] laid the foundation for the analyses. The mean levels of [oxyHb] during the last 10 s of the pre-task period was deemed baseline. The mean levels of [oxyHb] during the last 50 s task period of VFT-letter, VFT-category, and TOH, and the last 110-sec task period of the Sternberg task and the Stroop task were deemed activation levels, since stable elevation of [oxyHb] by task execution was observed 10 s after task initiation. The difference between activation and baseline levels was deemed size of activation (Δ[oxyHb]). Task protocols and procedures of data analysis in each task are shown in Fig. 1-c. Statistical analyses were carried out using the SPSS version 10 (SPSS Inc., Chicago, IL). Chi-square test for independence of group and gender, Mann–Whitney test for age, years of education, JART, task performance, were performed. Two designs of repeated-measures ANCOVA were performed. One design of ANCOVA (the design-1 ANCOVA) was performed to test Δ[oxyHb] for each task, using diagnosis group, gender, hemisphere, and task order as the factors, and age, education, and behavioral performance as the covariates. In the design-1 ANCOVA, diagnosis group was set as a factor since our main interest was group difference. Gender was included as a factor based on Kameyama et al. (2004) report of sex differences in cortical activation, as indicated by NIRS. As for the hemisphere factor, potential difference in NIRS activation has been reported in association with linguistic tasks and hemisphere dominance (Kubota et al., 2005). Since the total time of tasks could influence the results of cortical activation, task order was included as a factor. Moreover, age, education, and behavioral performance were set as the covariates since these variables could potentially affect neural activation. Another design of ANCOVA (the design-2 ANCOVA) was performed, using tasks, diagnosis group, gender, hemisphere, and task order as the factors, and age and education as the covariates. In the design-1 ANCOVA, Spearman's rank-correlation and multiple comparisons with Bonferroni's correction (Curtin and Schulz, 1998) were performed between Δ[oxyHb] and demographics and major clinical parameters for the tasks when significant group effects were found. For changes in [deoxyHb], repeated-measures ANCOVA was performed to test for differences between activation and baseline levels (Δ[deoxyHb]) for each task, using diagnosis group, gender, hemisphere, and task order as the factors, and age, education, and behavioral performance as the covariates. The level of significance was set at $p<0.05$.

3. Results

3.1. Performance data

The results for task performance for each task in both schizophrenia patients and healthy control groups are shown in Table 2. For all tasks, task performance was lower in schizophrenia than in healthy controls (Mann–Whitney *U* test).

3.2. NIRS data

The results of Δ[oxyHb] for each task (the design-1 ANCOVA) are shown in Fig. 2. For VFT-letter, the repeated-measures ANCOVA revealed significant difference for

Table 2
Performance data

	Schizophrenia (30)	Healthy controls (30)
VFT-letter	13.0±3.9**	17.4±3.8
VFT-category	23.7±5.0**	28.9±4.6
TOH	6.1±3.1**	11.0±3.6
(Schizophrenia 2/Healthy controls 11)[a]		
Sternberg task	20.8±2.8**	22.6±1.7
Stroop task	37.8±4.0*	39.6±0.7

Performance data are presented as mean±SD. VFT-letter, Verbal Fluency Test-letter; VFT-category, Verbal Fluency Test-category; TOH, Tower of Hanoi.
** $p<0.01$, * $p<0.05$; Mann–Whitney *U* test was used.
[a] Subjects to complete the task.

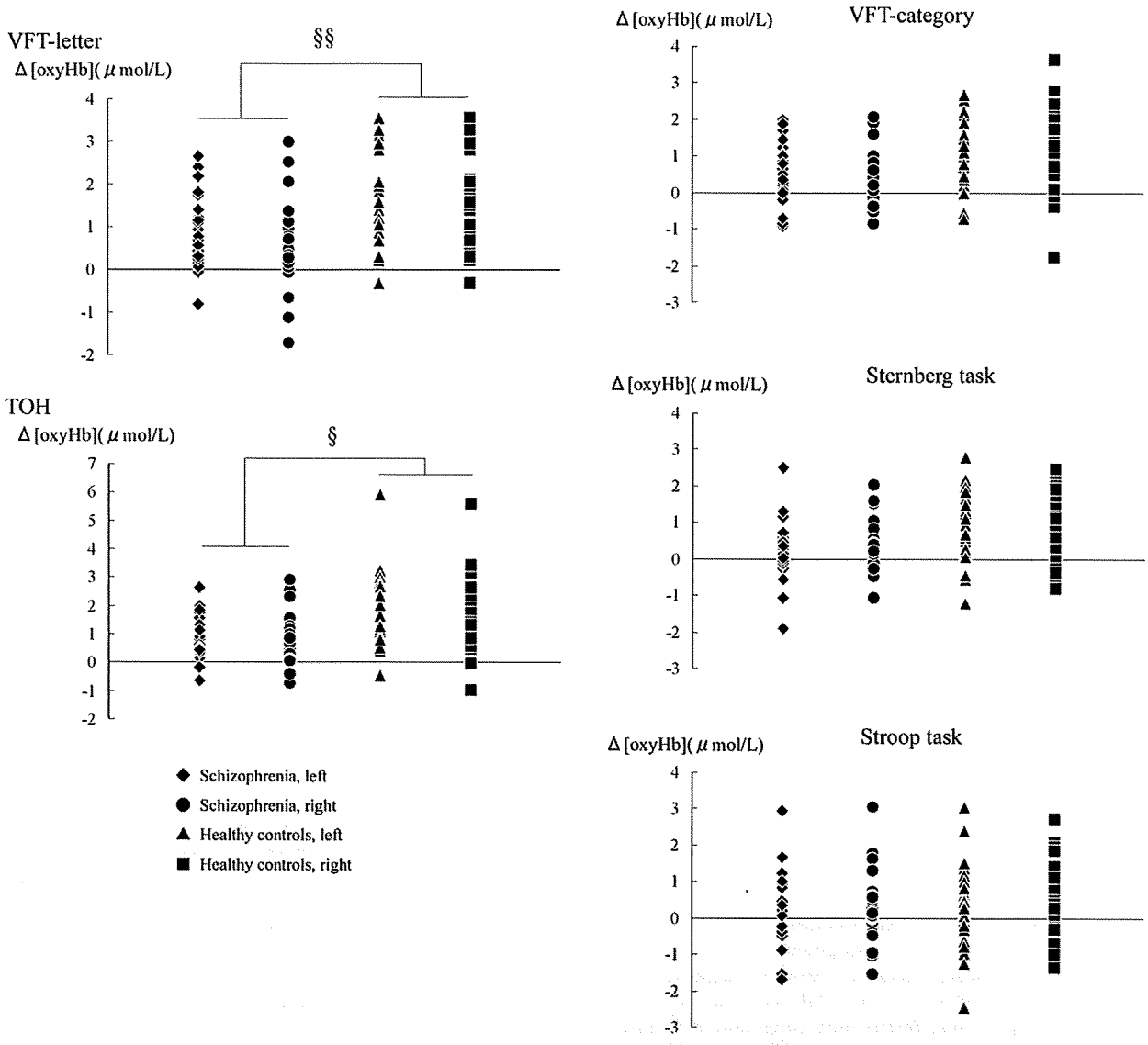

Fig. 2. The results of changes in [oxyHb] (μmol/L; Δ[oxyHb]) in five frontal lobe tasks. During VFT-letter and TOH, the repeated-measures analysis of covariance (the design-1 ANCOVA) revealed significant main effect of diagnosis group. During VFT-category, the Sternberg task, and the Stroop task, the design-1 ANCOVA revealed no significant main effect of diagnosis group. The effect size of each task was as follows: VFT-letter (left: 0.82, right: 0.88), VFT-category (left: 0.61, right: 0.77), TOH (left: 0.90, right: 0.86), the Sternberg task (left: 0.54, right: 0.61), the Stroop task (left: 0.04, right: 0.21). §§ $p<0.01$, § $p<0.05$; significant group effect VFT-letter, Verbal Fluency Test-letter; VFT-category, Verbal Fluency Test-category; TOH, Tower of Hanoi.

diagnosis group ($F(1, 58)=13.138$, $p<0.001$). Post-hoc analysis revealed that healthy controls exhibited a significantly larger increase in Δ[oxyHb] than schizophrenia patients. There was a significant main effect of task order ($F(1, 58)=9.148$, $p=0.004$). Post-hoc analysis revealed that an increase in Δ[oxyHb] in order A was significantly larger than in order B. Regarding TOH, the design-1 ANCOVA revealed a significant main effect for diagnosis group ($F(1, 58)=5.824$, $p=0.02$). Post-hoc analysis revealed that healthy controls exhibited a significantly larger increase in Δ[oxyHb] than schizophrenia patients. There was a significant interaction between diagnosis group and gender ($F(1, 58)=4.432$, $p=0.04$). The post-hoc analysis using Bonferroni's correction revealed that healthy controls showed a significantly larger increase in Δ[oxyHb] than schizophrenia patients in males ($p=0.003$), and male subjects showed a significantly larger increase in Δ[oxyHb] than female subjects in healthy controls ($p=0.016$). In VFT-category and the Sternberg task, the design-1 ANCOVA revealed no significant main effect of diagnosis group ($F(1, 58)=3.905$, $p=0.054$, $F(1, 58)=2.771$, $p=0.102$ respectively). For the Stroop task, the design-1 ANCOVA revealed no significant main effect of diagnosis group ($F(1, 58)=0.379$, $p=0.541$), but there was a significant main effect of task order ($F(1, 58)=8.810$, $p=0.005$). Post-hoc analysis revealed that an increase in Δ[oxyHb] in order B were significantly larger than in order A. Except for TOH, there was no interaction between factors for the tasks. The design-2 ANCOVA revealed a significant main effect of diagnosis group ($F(1, 58)=9.511$, $p=0.003$). The post-hoc analysis using Bonferroni's correction revealed a significant main effect of tasks (VFT-letter – Sternberg task; $p<0.001$, VFT-

Table 3
Spearman's rank correlation coefficients between Δ[oxyHb] and demographic, clinical data

	Schizophrenia(30)				Healthy controls(30)			
	VFL-l	VFL-r	TOH-l	TOH-r	VFL-l	VFL-r	TOH-l	TOH-r
Age	−0.14	−0.17	−0.27	−0.20	−0.11	−0.17	−0.30	−0.29
Years of education	−0.25	−0.15	0.07	0.01	0.05	0.01	0.35	0.39[a]
JART	0.23	0.20	0.45[a]	0.16	−0.09	−0.06	−0.04	0.02
Onset age	−0.19	−0.19	0.27	0.07				
Duration of illness	−0.11	−0.01	−0.48[a]	−0.25				
Equivalents of CPZ	0.00	−0.14	−0.11	−0.42[a]				
PANSS								
Positive symptoms	0.19	0.18	−0.34	−0.12				
Negative symptoms	0.07	0.02	−0.43[a]	−0.29				
General psychopathology	0.26	0.21	−0.27	−0.15				
Five-factor model of PANSS								
Positive	0.20	0.12	−0.33	−0.21				
Negative	0.01	−0.03	−0.39[a]	−0.21				
Cognitive	0.18	0.07	−0.52[a]	−0.53[a]				
Excitement	0.25	0.36	−0.17	0.19				
Depression/Anxiety	0.01	0.13	−0.10	0.08				

Correlation coefficients are presented using Spearman's rank correlation in both groups. JART, the Japanese version of the National Adult Reading Test; CPZ, chlorpromazine; PANSS, the Positive and Negative Syndrome Scale; DIEPSS, the Drug-Induced Extrapyramidal Symptom Scale. VFL-l, Verbal Fluency test Letter-left; VFL-r: Verbal Fluency test Letter-right; TOH, Tower of Hanoi.
[a] $p<0.05$.

letter – Stroop task; $p<0.001$, VFT-category – TOH; $p=0.011$, VFT-category – Stroop task; $p=0.014$, TOH – Sternberg task; $p<0.001$, TOH – Stroop task; $p<0.001$). The design-2 ANCOVA showed no interaction between any factors.

The results of Δ[deoxyHb] for each task are as follows. In the VFT-category, the repeated-measures ANCOVA revealed a significant main effect of diagnosis group ($F(1, 58)=7.545$, $p=0.008$). Post-hoc analysis revealed that healthy controls exhibited a significantly larger decrease in Δ[deoxyHb] than schizophrenia patients. For TOH and the Sternberg task, the repeated-measures ANCOVA revealed a significant main effect of diagnosis group (TOH: $F(1, 58)=5.957$, $p=0.018$; Sternberg: $F(1, 58)=6.297$, $p=0.015$), and post-hoc analysis revealed that healthy controls exhibited a significantly larger decease in Δ[deoxyHb] than schizophrenia patients. However, there was a significant interaction between diagnosis group and gender ($F(1, 58)=4.951$, $p=0.031$) only for TOH, with post-hoc analysis using Bonferroni's correction indicating a significantly larger decrease in Δ[deoxyHb] in healthy controls compared to schizophrenia patients in males ($p=0.002$), and a significantly larger decrease in Δ[deoxyHb] in male subjects compared to female subjects in healthy controls ($p=0.039$). Regarding VFT-letter and the Stroop task, the repeated-measures ANCOVA revealed no significant main effect of diagnosis group ($F(1, 58)<0.001$, $p=0.989$, $F(1, 58)=2.328$, $p=0.133$ respectively). In the Stroop task, we found a significant effect of task order via the repeated-measures ANCOVA ($F(1, 58)=8.972$, $p=0.004$). Post-hoc analysis revealed that a decrease in Δ[deoxyHb] in order B was significantly larger than in order A. There was no interaction between factors, except for TOH.

3.3. Correlation

For VFT-letter and TOH, in which a significant main effect of diagnosis group was revealed by the repeated-measures ANCOVA (the design-1 ANCOVA), the correlation between Δ[oxyHb] and demographic and clinical parameters was analyzed using Spearman's rank-correlation. These results are shown in Table 3. In schizophrenia patients, left Δ[oxyHb] during TOH showed a significant positive correlation with JART (rho=0.45) and a significant negative correlation with illness duration (rho=−0.48). Right Δ[oxyHb] during TOH correlated negatively with chlorpromazine (CPZ) equivalents (rho=−0.42). Left Δ[oxyHb] during TOH also showed a significant negative correlation with negative symptoms scores on PANSS (rho=−0.43) and with negative (rho=−0.39) and cognitive symptoms scores on the five-factor model of PANSS (rho=−0.52). Similarly, right Δ[oxyHb] during TOH showed a significant negative correlation with cognitive symptoms scores on the five-factor model of PANSS (rho=−0.53). During VFT-letter, no significant correlation was found between Δ[oxyHb] and any of the variables in the analyses. Further analysis of multiple comparisons showed that these correlations between Δ[oxyHb] during TOH and clinical parameters in schizophrenia were not statistically significant.

4. Discussion

In this study, we measured PFC activity during four well-established frontal lobe tasks, namely VFT, TOH, the Sternberg, and the Stroop task, using a 2ch-NIRS system. Our findings indicate a significant main effect of diagnosis group for VFT-letter and TOH as analyzed Δ[oxyHb] by the repeated-measure ANCOVA (the design-1 ANCOVA). Further analysis of the correlation between clinical parameters and Δ[oxyHb] revealed that left Δ[oxyHb] during TOH showed a significant negative correlation with negative symptoms scores on PANSS and with negative and cognitive symptoms scores on the five-factor model of PANSS for schizophrenia patients. However, no significant correlation was found between Δ[oxyHb] and any clinical parameters during VFT-letter. In the design-2 ANCOVA, a significant main effect of diagnosis group was recognized.

4.1. OxyHb data

The use of a 2ch-NIRS system to evaluate PFC activation during VFT was considered appropriate based on findings